August 2001

Mesoscale oceanographic data analysis and data assimilative modeling with application to Western Australian fisheries

Dr David Griffin

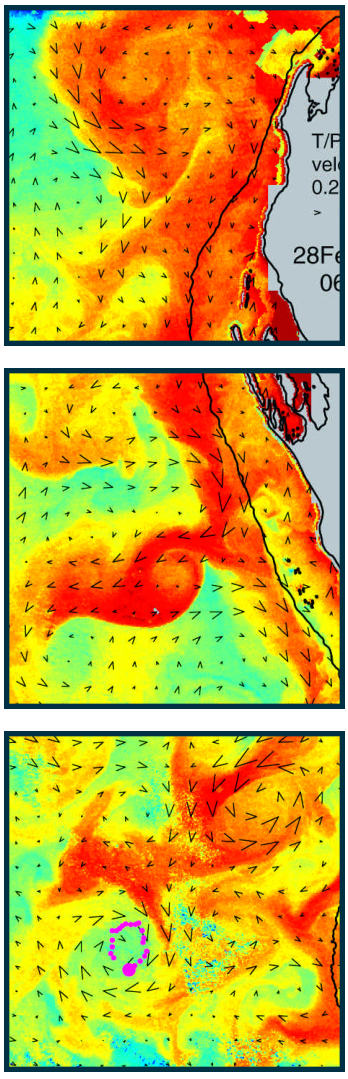

FRDC Project 97/139

CSIRO MARINE RESEARCH
FISHERIES WESTERN AUSTRALIA
NIWA

Mesoscale oceanographic data analysis and data assimilative modelling with application to Western Australian fisheries.

Bibliography.
ISBN 1 876996 01 3.

1. Fishery resources - Western Australia. 2. Oceanography - Western Australia. 3. Lobsters - Western Australia - Larvae. 4. Lobster fisheries. I. Griffin, David A. II. CSIRO. Marine Research. (Series : FRDC Project ; no. 1997/139).

639.209941

Mesoscale oceanographic data analysis and data assimilative modelling with application to Western Australian fisheries.

David A Griffin[A], John L Wilkin[B], Chris F Chubb[C], Alan F Pearce[D] and Nick Caputi [E]

[A]*CSIRO Marine Research, GPO Box 1538, Hobart, Tas 7001.*
David.Griffin@marine.csiro.au

[B]*National Institute of Water and Atmospheric Research, New Zealand, now at Institute of Marine and Coastal Sciences, Rutgers University, New Jersey USA.*
wilkin@imcs.rutgers.edu

[C] *Western Australian Marine Research Laboratories, Fisheries WA, PO Box 20, North Beach WA 6920.* cchubb@fish.wa.gov.au

[D]*CSIRO Marine Research, PO Box 20, North Beach WA 6920.*
Alan.Pearce@marine.csiro.au

[E] *Western Australian Marine Research Laboratories, Fisheries WA, PO Box 20, North Beach WA 6920.* ncaputi@fish.wa.gov.au

August 2001
CSIRO Marine Research

ISBN 1 876996 01 3

FRDC Project No. 1997/139

Table of Contents

Table of Contents 3
OUTCOMES ACHIEVED 4
Acknowledgments 7
Background 7
Need 9
Objectives 10
Near-surface currents and temperatures from satellite altimetry and thermometry 10
Methods 10
Altimetry 10
Thermometry 12
Results 13
Three-dimensional data-assimilating model 17
Methods 17
Results 23
Discussion 29
Larval advection model 30
Methods 30
Results 34
Discussion 44
Benefits 46
Further Development 46
Planned Outcomes 47
Conclusion 47
References 49
Appendix 1: Intellectual Property 52
Appendix 2: Staff 52
Appendix 3: Ocean currents from successive satellite images: the reciprocal filtering technique. 52
Appendix 4: WA ocean movies 1993-2000 52
Appendix 5: WA ocean model movies 1995-1998. 52

1997/139 Mesoscale oceanographic data analysis and data assimilative modelling with application to Western Australian fisheries.

PRINCIPAL INVESTIGATOR: Dr David A Griffin
ADDRESS: CSIRO Marine Research
PO Box 1538
Hobart Tas 7001
Telephone: 03 6232 5244 Fax: 03 6232 5000

OBJECTIVES:

1. To develop algorithms for operational estimation of near-surface currents and temperatures off south-western Australia based on satellite altimetry and thermometry.
2. To develop and test a three-dimensional data-assimilating model of ocean dynamics off Western Australia, to be run in hindcast mode, archiving data for the last ten years.
3. To run tracking scenarios for rock lobster larvae to describe larval behaviour under different environmental conditions (extended to other larvae as time permits).
4. To provide advice on management issues that may be addressed by improved ocean understanding, such as the spawning locations of successful larvae, and correlations between larval success and ocean conditions.

NON TECHNICAL SUMMARY:

OUTCOMES ACHIEVED

1) It is more widely recognized within the Australian community (both scientific and general) that satellite altimetry can be used to produce accurate maps of the surface circulation of the ocean. It is still too early for the outcomes of this to be apparent, but we assume they will be significant.

2) The basic mechanism responsible for movement of larvae of western rock lobster offshore and their return to the coast is much better understood. This understanding has been communicated to fishers who received the information enthusiastically. We expect that this common understanding of the recruitment process will further increase the (already high) level of cooperation of the industry with research and management.

3) Researchers and managers of the western rock lobster fishery have increased confidence in the assumption that the probability of larval survival and subsequent settlement is independent of the location of hatching. Hence, the management objective will continue to be that the breeding stock in all areas is protected equally. That this objective is supported by research can only protect the fishery's Marine Stewardship Council certification.

4) With regard to the question of why El Nino is associated with very poor levels of larval recruitment, attention has been shifted from the direct influence of ocean currents in transporting larvae to the indirect influences on their growth and mortality.

The more that is understood about the factors controlling the abundance of an exploited fish stock, the more optimally it can be harvested for sustainable yield and profit. It has been known for some time that catches of western rock lobster are closely related to the number of larvae surviving their year at sea and settling as puerulus on the coast, and that the variation in settlement, in turn can be statistically predicted using several types of ocean data. What is not understood is why sea level, for example, should be a predictor of larval survival. This needs to be understood so that insight into reasons why the correlation might break down (as it did in 1998) can be gained, and so that a better predictor can be found. The value of a reliable indicator of the environmental influence on larval survival is that, for example, a year of very poor larval settlement can then be correctly attributed to either over-fishing of the breeding stock, or poor survival rates at sea.

This project addressed the question of why larval survival rates are so variable by taking a process-based, modelling approach, as distinct from the statistical, or correlative approaches taken to date. The modelling approach has only recently become feasible, for two reasons. One is that the computing demands are high, but the more significant recent advance is the advent of satellite techniques for mapping near-surface ocean currents. We used these maps to calculate where winds and ocean currents from 1993 to 1998 carried numbers of individual western rock lobster larvae, from hatching to far offshore, then back to the coast.

Crucial to the success of this project was that relatively much has been learnt, from decades of sampling from ships, about the behaviour of larval western rock lobsters in the deep ocean. In particular, we needed to know the details of when larvae rise to the surface and when they descend to depth, and how this varies with larval age, time of day, phase of moon, etc. We also needed to know what triggers a late-stage larva to metamorphose to the non-feeding, fast-swimming puerulus stage that is found settling on inshore reefs. This trigger, however, is unknown, so our model simply assumes that all larvae at least 270 days old make this transition if they find themselves over the continental slope near new moon, a behaviour that is consistent with available observations.

In the first phase of the project, many types of ocean data were assembled, and two techniques developed for making accurate maps of the ocean currents. The first technique was relatively straightforward: observations of sea level height and surface temperature were used to estimate the surface currents directly via approximations of the physical equations. The second technique is called data-assimilative modeling. The satellite data were ‘assimilated’ into a hydrodynamic model.

Our data-assimilating model of the ocean currents of Western Australia is the first of its kind in Australia. However, it took somewhat longer to complete than originally planned, and we still consider it to be a work in progress. Work on this model was de-prioritised in favour of using the maps of ocean near-surface currents diagnosed directly from the satellite data, which turned out, fortunately, to be more accurate than hoped for. The accuracy of these ‘altimetric’ current maps was assessed by comparing them with the velocities of satellite-tracked drifting buoys, and animations of ocean thermal imagery.

The current maps and (also only recently available digitally) daily wind maps were then combined with information on larval behaviour and many simulations were performed of the fate of six year-classes of lobster larvae. The simulations confirm the importance of the summer southerly winds in transporting larvae 'upstream' against the mean onshore and southward flows that exist just below the surface, and which help return larvae to the coast. The simulations also highlight the role of energetic eddies, which mix the larvae at velocities much in excess of the larger-scale flows.

It is the vigorous mixing by eddies in our simulations that produce the result that the location of hatching of larvae quickly becomes immaterial to its destiny. To test this hypothesis was one of our primary objectives because of its relevance to the potential benefit of preferentially protecting certain spawning regions.

With regard to explaining the observed correlation of sea level with larval settlement, our simulations confirm that sea level does serve as an indicator of both the strength of the Leeuwin Current, and the intensity of eddies associated with it, but does not support the hypothesis that the direct (transporting) influence of the currents on the larvae is responsible for the large (ie five-fold) changes observed in how many return to the coast.

So the mystery of why larval settlement correlates with sea level remains, although we now have a clearer picture of how any return at all.

We concluded our project with a very preliminary study of the potential importance, to larval survival, of the inter-annual variability of food availability. For this we used the recently launched SeaWiFS satellite that senses ocean colour, from which near-surface chlorophyll abundance can be estimated. These data show that there was less phytoplankton in the water in the summer of 1997-98 than in the next two summers, perhaps explaining why the settlement in 1998 was very low, even though the prediction based on sea level was for average settlement.

The next step to take is to include temperature- and prey field-dependent larval growth and mortality in an advection model such as the one developed here. In addition to explaining the inter-annual variability of settlement, the inclusion of growth and mortality in the model could also change our finding about the importance of hatching location, because of the regional differences that exist in primary production.

To complete this project, we have produced an educational CD-ROM with all the data assembled, along with results of the larval transport simulations, presented in the form of movies that can be viewed on any computer. The CD can be browsed at www.marine.csiro.au/~griffin/WACD/index.htm.

KEYWORDS: Western Rock Lobster, larval advection, ocean currents, altimetry, data assimilation.

Acknowledgments

This project relied heavily on data provided mostly free of charge by other agencies. We are grateful to the NASA Physical Oceanography Distributed Active Archive Center at the Jet Propulsion Laboratory / California Institute of Technology for altimetric sea level height data from the European Space Agency ERS and NASA-CNES Topex/Poseidon missions, the Western Australian Department of Transport and the National Tidal Facility for tide gauge data, the US National Oceans and Atmospheric Administration (NOAA) and Western Australian Satellite Technology and Application Consortium (WASTAC) for Advanced Very High Resolution Radiometer thermal imagery data, the US National Center for Atmospheric Research and the National Center for Environmental Prediction for wind velocity and stress estimates, NASA-GSFC (Goddard Space Flight Centre) for SeaWiFS chlorophyll-a 8-d composites, the Bureau of Meteorology for wind data from Fremantle, the NOAA Atlantic Oceanographic and Meteorological Laboratory and the Canadian Marine Environmental Data Service (MEDS) for interpolated (Krig) drifter data from the World Ocean Circulation Experiment Surface Velocity Program and the Australian Geological Survey Organisation for detailed bathymetric data.

Background

The Leeuwin Current is the dominant oceanographic feature along the Western Australian Coast. It brings warm, nutrient-depleted waters southward in a powerful, turbulent stream that meanders along the continental slope, sometimes veering off to sea to accumulate in large anticyclonic eddies (Cresswell and Golding, 1980, Godfrey and Ridgway, 1985, Andrews, 1983, Pearce and Griffiths, 1991). The strength of the current is strongly modulated on both seasonal and inter-annual timescales. It is strongest in winter, and especially so in extended La Nina periods. Conversely, it is weakest in summer and can stop altogether during an El Nino. When this occurs, the summer southerly winds can more easily drive upwelling, which the Leeuwin usually suppresses, dropping surface temperatures considerably.

The Leeuwin Current has a profound influence on all Western Australian marine life. Without it, the ecosystem of Western Australia would be much more temperate than sub-tropical. The variability of the Leeuwin sends shocks through the marine communities. Some do better when it is weak, while others prefer it to be strong (Lenanton, 1991, Caputi *et al.*, 1996).

Western rock lobster (*Panulirus cygnus* George), the major commercial fishery of Western Australia, has a strong preference for a strong Leeuwin Current. The larval period is clearly the critical phase, with recorded numbers of settling pueruli being about five times greater in some years than others, translating to a factor of 1.5 or so in the tonnage caught by the fishery three to four years later (Phillips, 1986). Why this should be so is unknown, although it is thought (Pearce and Phillips, 1988) that the increased strength of the current is beneficial in returning larvae onshore and southward, countering the effect of summer southerly winds that take them northwestward. Alternatively, the

increased temperature is known to speed development. This might also convey a survival benefit (Chittleborough and Thomas, 1969).

It is assumed that the strength of the Leeuwin Current can be inferred from Fremantle sea level. Direct measurements of the flow of the Leeuwin Current are far too few for any studies of the impact of its variability. All we *really* know is that recruitment of many species is correlated (some positively, some negatively) with coastal sea level, an ocean variable of unlikely biological significance, but which happens to be very easy to measure.

Advances in ocean observing systems and numerical modeling are opening our eyes to what is happening in the open ocean ecosystem. We are still a long way from being able to accurately hindcast all ocean variables, but progress in that direction is steady. The first two objectives of this project were to apply current state-of-the-art ocean observing and modeling techniques to the ocean off Western Australia, in order to provide a suite of tools for exploring hypotheses of the role of physical oceanographic processes on Western Australian fisheries.

The most recent major advance in ocean observation is the advent of satellite-borne altimetry. Satellite altimetry measures sea level along intersecting lines all over the globe. Sea level is to an oceanographer what barometric pressure is to a meteorologist, so having maps of sea level instead of just point measurements at the coast is just like having a weather map instead of just a single barometer. The altimeter, however, was not (at the beginning of this project) a proven technology. Nor was it designed specifically for regional applications. Its primary mission was to monitor large-scale ocean phenomena like El Nino. To make up for anticipated deficiencies of altimetry at the meso- and regional (30km-1000km) scale, our first objective was to develop techniques of combining the altimetry data with sea surface temperature data in order to make accurate maps of surface currents. The second objective, both a back-up and extension of the first, was to exploit recent advances in ocean modeling whereby data are used not just for comparison with the model, but actually to force the model to mimic reality more closely. This is known as data-assimilative modeling, and while it is currently how weather forecasts are produced, it is still an unproven technology for ocean meso-scale applications.

The third objective was to model the trajectories of rock lobster larvae, to see if the observed variability of puerulus settlement could be explained using the new ocean current information resulting from the first two objectives. This was to be achieved by developing a process-based, rather than statistical, model of the impacts of environmental variability on the fate of the larvae. As a result of decades of field sampling, relatively much is known about how the spatial and depth distribution of the larvae of western rock lobster varies diurnally and through the year. But that information does not explain how the larvae came to be distributed as observed, or which of those larvae sampled had much of a chance of returning to the fishery. Chittleborough and Thomas (1969) speculated that larvae were transported offshore under the influence of the strong southerly winds prevailing through the summer, when hatching occurs. How the larvae returned back to

the coast was unclear, although the potential importance of a mean eastward flow beneath the wind-driven Ekman layer was considered. The existence of a mean geostrophic eastward flow is no longer questioned, but no one has attempted to construct a quantitative, mechanistic model of how the observed, age-dependent, diel vertical migration behaviour of the larvae interacts with the seasonal and vertical differences in the current velocities in order to return larvae to the population. Our objective was to do just this, and then to see if the *inter-annual* variability of the currents explains the inter-annual variability of larval settlement. We refer to this model as a 'larval advection model', because advection was the only process modeled quantitatively. By this we mean that other processes, such as mortality and growth, were not included. Hence, of all the hypotheses that have been put forward to explain the correlation of puerulus settlement with sea level, we proposed only to test the one that recent advances in ocean observing and modeling have made it feasible to test.

There are two main managements needs for a greater understanding of the larval phase. The first stems from the fact that the stock-recruitment relationship for western rock lobster is extremely noisy. This makes it harder to set optimal egg production targets from year to year, and later, to assess whether raising or lowering those targets did, in fact, have the desired impact. This need can only be addressed if the noise in the stock-recruitment relationship can be explained. For western rock lobster, the 'noise' actually dominates the signal, so being able to explain the noise is important. The goal of this project is to take us closer to a mechanistic, rather than correlative, explanation of the environmentally-driven component of the 'noise' in the stock-recruitment relationship.

Need

The correlation of western rock lobster larval settlement with sea level is of great value to the managers of the fishery, even if the reason for the correlation is unknown. If larval settlement is poor when sea level is low, they know there is less need to take management action than if the same occurs when sea level is high, which would then indicate that perhaps measures need to be taken to increase the breeding stock. The correlation of sea level with settlement, however, is far from perfect. Including onshore winter wind (as inferred from rainfall) in the equation improves the correlation. But there is still a need for a better indicator of the environmental influence on the probability of survival of larval lobsters. Confidence in the real (rather than coincidental) skill of this indicator will be greatest if it is known *why* it correlates with larval survival.

A second management need for a greater understanding of the larval recruitment process is with regard to the questions of zoning and stock structure. It is presently assumed that mixing of larvae is complete and that all zones contribute to recruitment in proportion to their egg production, and that recruitment in each zone may be derived from all others. Is this assumption valid? Or are there sections of the breeding stock that consistently provide significant proportions of the puerulus settlement each season?

Objectives

- To develop algorithms for operational estimation of near-surface currents and temperatures off south-western Australia based on satellite altimetry and thermometry.
- To develop and test a three-dimensional data-assimilating model of ocean dynamics off Western Australia, to be run in hindcast mode, archiving data for the last ten years.
- To run tracking scenarios for rock lobster larvae to describe larval behaviour under different environmental conditions (extended to other larvae as time permits).
- To provide advice on management issues that may be addressed by improved ocean understanding, such as the spawning locations of successful larvae, and correlations between larval success and ocean conditions.

Near-surface currents and temperatures from satellite altimetry and thermometry

Methods

Altimetry

The NASA-CNES Topex/Poseidon (T/P) satellite was launched in September 1992. At that time it was unclear how precise the measurements would be, since a host of corrections to the raw data from the satellite needed to be made. In the following years, techniques were developed by the Science Working Team, of which CSIRO is a member, for processing the raw data to usable estimates of sea level. For this project, we used the Geophysical Data Records distributed by NASA-JPL, consisting of estimates of sea level at 7km intervals along the sub-satellite track. The precision of these measurements is now believed to be as small as 1.5cm (a third of the design figure), averaged over the globe.

The European Space Agency (ESA) Earth Resources Satellite (ERS), launched earlier, also carries an altimeter, but the satellite's orbit is less precisely tracked than that of T/P. Hence, the ERS data only became of real use when merged with T/P data.

T/P is in an orbit which takes 10 days to completely re-sample a grid of tracks that are separated by 250km at mid-latitudes, while ERS takes 35 days to re-sample tracks separated by 160km at mid-latitudes. Appendix 4 includes an animation of the track sampling sequence. We combine the data from both satellites by optimally interpolating the data onto a regular 0.1758° grid (latitude and longitude – about 19.5km N/S by 16.5km E/W) spanning 41.9°S to 21.1°S, 100.1°E to 124.9°E, every 5 days, with overlapping data-windows of 25 days.

The adequacy of this combined sampling rate depends on how rapidly sea level changes in the region of interest, at the length-scale of interest. Near the coast, it is known from tide gauge records that sea level changes significantly from day to day, even after the tides are removed, due to wind forcing. Thus, altimetry was not expected to have an

adequate sampling rate to monitor all the variability over the shelf. Much less was known about the spectrum of sea level variability in the open ocean prior to altimetry because no other observations existed. Nevertheless, it was not expected that just one or even two altimeters would suffice to adequately sample the meso-scale features such as boundary currents and their eddies. Hence, to simply interpolate all data within a 25 day window onto a single map with 20km resolution was potentially a waste of time.

Our mapping process included three stages; 1) along-track interpolation with an averaging-scale of 50km, 2) two-dimensional mapping with a long (130km) averaging scale to provide estimates between tracks, then 3) two-dimensional mapping with short (50km) averaging scale to retain detail near tracks. These maps are of anomalies about the 1993-1998 mean, since the present estimate of the geoid is not accurate enough to estimate the mean height field at 20km resolution.

Coastal tide gauge data and estimates of the sea level anomaly at the shelf break were included in the sea level mapping. The shelf break estimates were formed by making the across-shelf height gradient (and hence the alongshore geostrophic current) a function of local and upstream (in the sense of coastal trapped wave propagation) alongshore wind stress. The other effect of doing this was to concentrate the height gradient associated with the Leeuwin Current over the continental slope, where we know, from observations, the axis of the current is most likely to be. The relationship of wind-driven shelf currents to local and remote wind forcing was established by a multiple regression analysis similar to that of Griffin and Middleton (1991). Note that the remote winds were certainly worth including in this procedure: tropical-cyclone force winds as far north as 15°S make a significant contribution to the shelf current at Fremantle (33°S).

We estimated the Cartesian components u,v of the altimetric current velocity $\mathbf{v}_{altim}$ from the sea level height η maps by assuming a steady-state, frictional, cyclostrophic momentum balance

$$-fu = g\eta_y + uv_x + vv_y + C_D(u^2+v^2)^{1/2}v/h \quad (1)$$

$$fv = g\eta_x + uu_x + vu_y + C_D(u^2+v^2)^{1/2}u/h \quad (2)$$

where f is the Coriolis parameter, g is the acceleration due to gravity, u and v are layer-averaged velocity components along the x and y axes, subscripts denote partial differentiation, $C_D=5\times10^{-4}$ is a drag coefficient and h is the layer thickness, estimated as $h=150+150\eta$. To solve (1) and (2), we estimated the terms on the RHS using the Cartesian components of the geostrophic altimetric velocity vector estimate $\mathbf{v}_{ga}$ given directly by

$$f\mathbf{v}_{\mathrm{ga}} = -g\nabla\eta \quad (3)$$

as approximate estimates of u and v. The effect of including the advective terms in (1) and (2) was to increase the velocities of anticyclonic flow, and decrease the velocity of cyclonic flow, for equal height gradient. The effect of including the frictional terms was

to make cyclonic eddies weakly convergent at the surface, and anticyclonic eddies divergent. The combined effect was to make changes of typically 10% of the total. The result that cyclonic eddies are convergent at the surface is supported by the drifter trajectories. WOCE drifter 6152 became trapped in a cyclonic eddy (with a central depression of 0.3 m) at 33°S, 113°E on 5 September 1995. The drifter remained in the eddy for at least 225 days, the data record ending at 34°S 105.5°E. Appendix 4 shows examples of other drifters that were also drawn to the center of cyclonic eddies, but no examples of drifters being drawn to the centres of anticyclonic eddies, although many orbits around those eddies were made.

Thermometry

We investigated two methods of augmenting altimetry with thermometry in order to estimate surface currents. Both were de-prioritised as components of the present project so they are discussed only briefly here.

The first approach attempted to exploit the fact that at certain length- and time-scales, sea level and temperature are positively correlated, simply because warm water is less dense than cold. Hence, temperature imagery should be useful for helping to interpolate the relatively sparse along-track altimetric observations onto the regular grid. Results, however, were disappointing so we will omit the details of the methods used. We think the approach fails because 1) the quantitative relationship of temperature to sea level is too variable to be of practical use in a simple scheme, and 2) algorithms for clearing cloud and warm-skin effects from satellite thermal images are not yet advanced enough for the remaining errors to be sufficiently small.

The second approach attempts to estimate current velocities directly from the satellite thermal images by tracking the movement of identifiable features from one image to the next. This method certainly has promise but there is still much developmental work to do before it can be used as a data source for other applications. A major limitation of the method is that it needs persistently clear skies. A second limitation is that many spurious velocity vectors are produced as well as good vectors, because automatic pattern-matching methods make many mistakes. To address the latter, we developed (see Appendix 3) a novel method of screening the spurious vectors by simply reversing the order in which image pairs are processed, and only accepting those vectors that are common to both analyses. The development of a method to combine the remaining good vectors with the altimetric estimates is still in its infancy.

Results

The altimetry results were so pleasing and generated so much interest that we have produced an educational CD-ROM, written for general audiences, that we are sure will also be a great resource for other scientists. The CD (see Appendix 4) has several types of movies on it, showing ocean surface environmental data (altimetric currents, satellite-derived temperatures, etc) for 1993 to 2000, so we have not included many plots here of the altimetric current velocities, but focus instead on how we decided that the altimetric velocities were of real value to the present project.

We evaluated and fine-tuned the altimetric method of measuring the surface currents by comparing (see Fig. 1) the altimetric estimates with 13,519 observed velocities of satellite-tracked drifting buoys and 363 research-vessel-borne Acoustic Doppler Current Profiler current velocity observations. The correlation coefficient of the altimetric and *in situ* estimates is 0.7 for both east-west and north-south velocity components. The regression coefficients are 0.41 and 0.47, respectively. This systematic under-estimation is due to the fact that the sea level mapping procedure, and gradient determinations, necessarily smooth out, on average, the true field. The root-mean-squared difference of the estimates is 0.24m/s for both components, while the root-mean-square of the altimetric and *in situ* estimates are 0.2m/s and 0.33m/s, respectively, for both components. Hence, the altimetric estimates account for about half of the variability of the *in situ* observations. Estimates in regions of strong (>1m/s) currents have a small (20%) relative error while estimates in regions of weak (<0.2m/s) currents are of less value, because the size of the errors is essentially independent of the *in situ* estimate of the current speed.

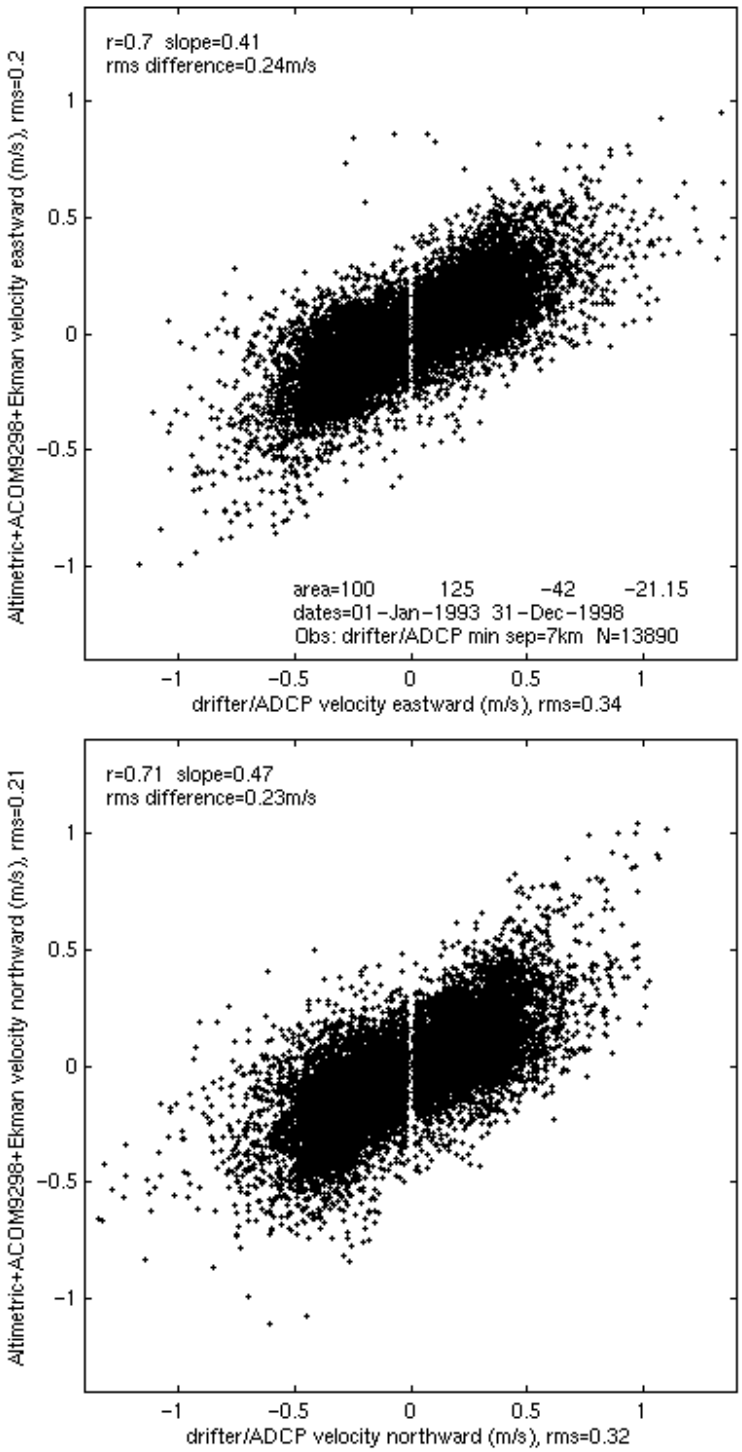

Figure 1 Comparison of *in situ* measurements of current velocity with corresponding 'model' estimates. The observed eastward (upper panel) and northward (lower panel) velocity components are plotted along the *x* axis and comprise 13519 WOCE drifter and 363 ADCP observations. The drifter velocities are those estimated at 6-hour intervals by the WOCE SVP DAC from interpolated trajectories, excluding estimates within 7km of each other. The drifters' drogues are centred at 15m. ADCP data are from *Franklin* cruises Fr95/3, Fr95/8 and Fr96/6 and are averaged between 20m and

28m depth for 20 minutes. Corresponding 'model' estimates for the time and place of the observations are plotted on the *y* axis. The 'model' is the sum of the satellite altimetric velocity, the mean velocity for 1992-1998 from the ACOM global model, and a simple Ekman layer model driven by daily NCEP Reanalysis winds. Root-mean-squares of observed, modeled and error velocities are given, as well as correlation and regression coefficients ('r' and 'slope', respectively).

We also found it instructive to compare our velocity estimates with six years of NOAA AVHRR images of sea surface temperature (SST), particularly when these are viewed as an animation. The comparison is very encouraging, although difficult to quantify. The altimetric estimates are clearly a smoothed version of reality, but most major flows are represented, and no 'spurious' eddies or currents seem to occur. In Fig. 2 is shown one example image (while Appendix 4 has hundreds more). The inclusion of drifters in the animations show that position errors are relatively small; their motion agrees better with the SST maps than do the altimetric estimates. The drifters often travel along sharp temperature fronts. For example, note the sharp temperature front along 29°S between 110°E and 112°E. This appears to result from a branch of the Leeuwin Current, that can be seen heading seaward from the continental slope along 28°S, riding over northward flow that must be associated with a gradient between high sea level at 29.5°S, 110°E and low sea level at 29.5°S, 112.5°E. The altimetric velocity field clearly lacks sharp frontal features such as this one, but does have the general sense of the circulation correct, right down to the meso-scale (see, for example, the drifter circling an eddy, centred near 34°S 111°E), which is a huge advance on what is possible without altimetry.
.

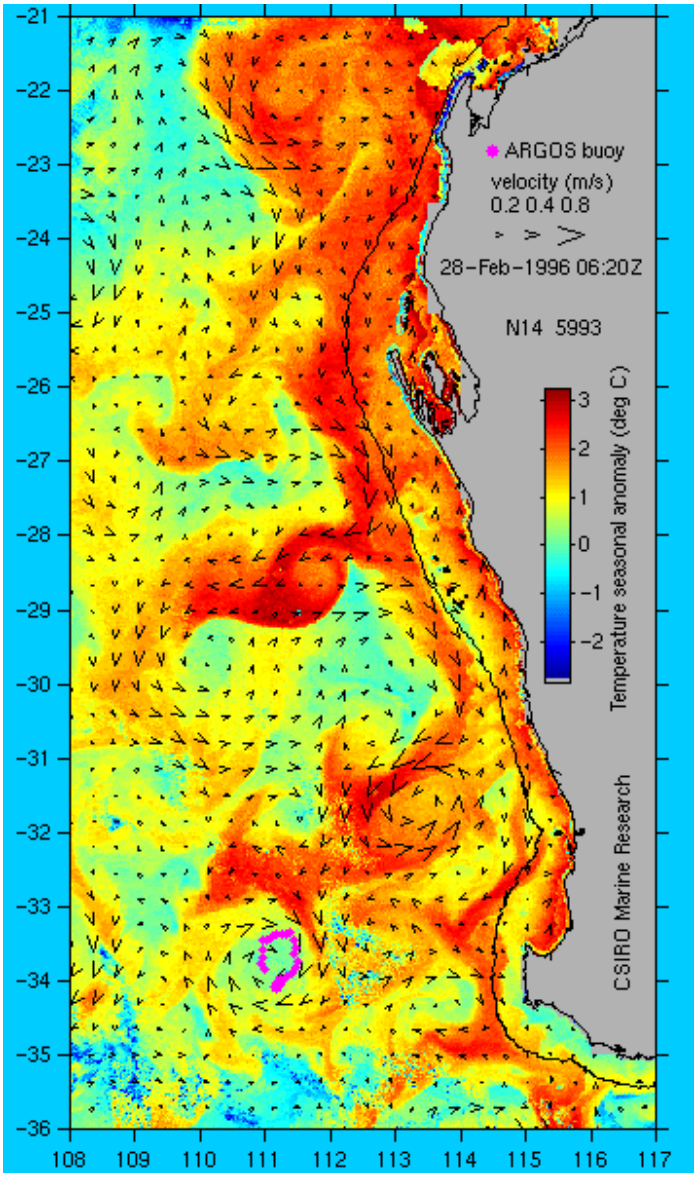

Figure 2 Comparison of altimetric current velocity estimates (arrow heads) with the trajectory, at 6-hour intervals over 5 days, of an Argos-tracked WOCE SVP surface drifter (in magenta) and sea surface temperature anomaly. The altimetric velocity has the time-mean velocity from the ACOM global model added. The SST anomaly is the difference of SST from the CSIRO Atlas of Regional Seas (CARS) seasonal (mean plus annual and semi-annual), climatological hydrographic SST field. The 200m isobath is shown.

Three-dimensional data-assimilating model

Methods

The three-dimensional hydrodynamic model constructed for this project is an implementation of the Regional Ocean Modeling System (ROMS). ROMS is the successor to the s-coordinate Rutgers University Model (SCRUM) nominated in the proposal and features a number of substantial technical improvements.

The model grid has 128×64 (latitude $\times$ longitude) nodes in the horizontal, spanning 22°S-37°S, 106°E-116°E. This gives a horizontal resolution of about 13km×15km. The vertical grid is terrain-following, with 20 nodes in the vertical spanning the local water depth as shown in Fig. 3 and 4, which show the uppermost 1000m and the full depth, respectively.

To prevent various computational problems, the water depth in the model must be a smoothed version of reality. The shallowest water in the model is 50m and the deepest is 5040m. Figures 5 and 6 compare the modeled topography with reality. Note how the narrow shelf off Perth has had to be broadened, and how the Abrolhos Islands have caused the model topography to veer offshore and back. To ensure computational stability, the only alternative to such 'earthworks' is to substantially reduce the grid intervals, which comes at a very high computational cost.

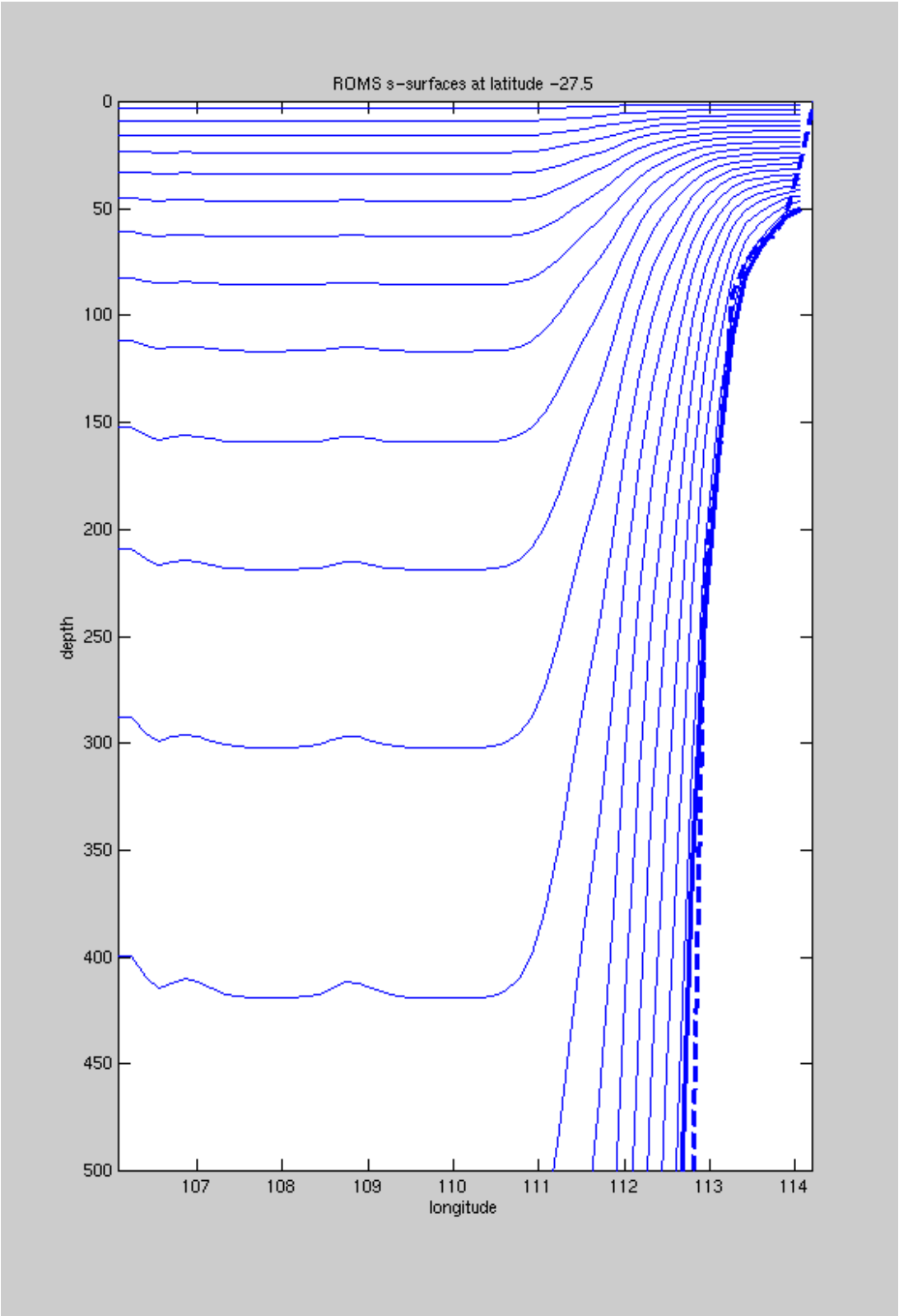

Figure 3 A vertical slice through the model grid at 27° 30' S, showing how vertical resolution becomes finer in shallow water.

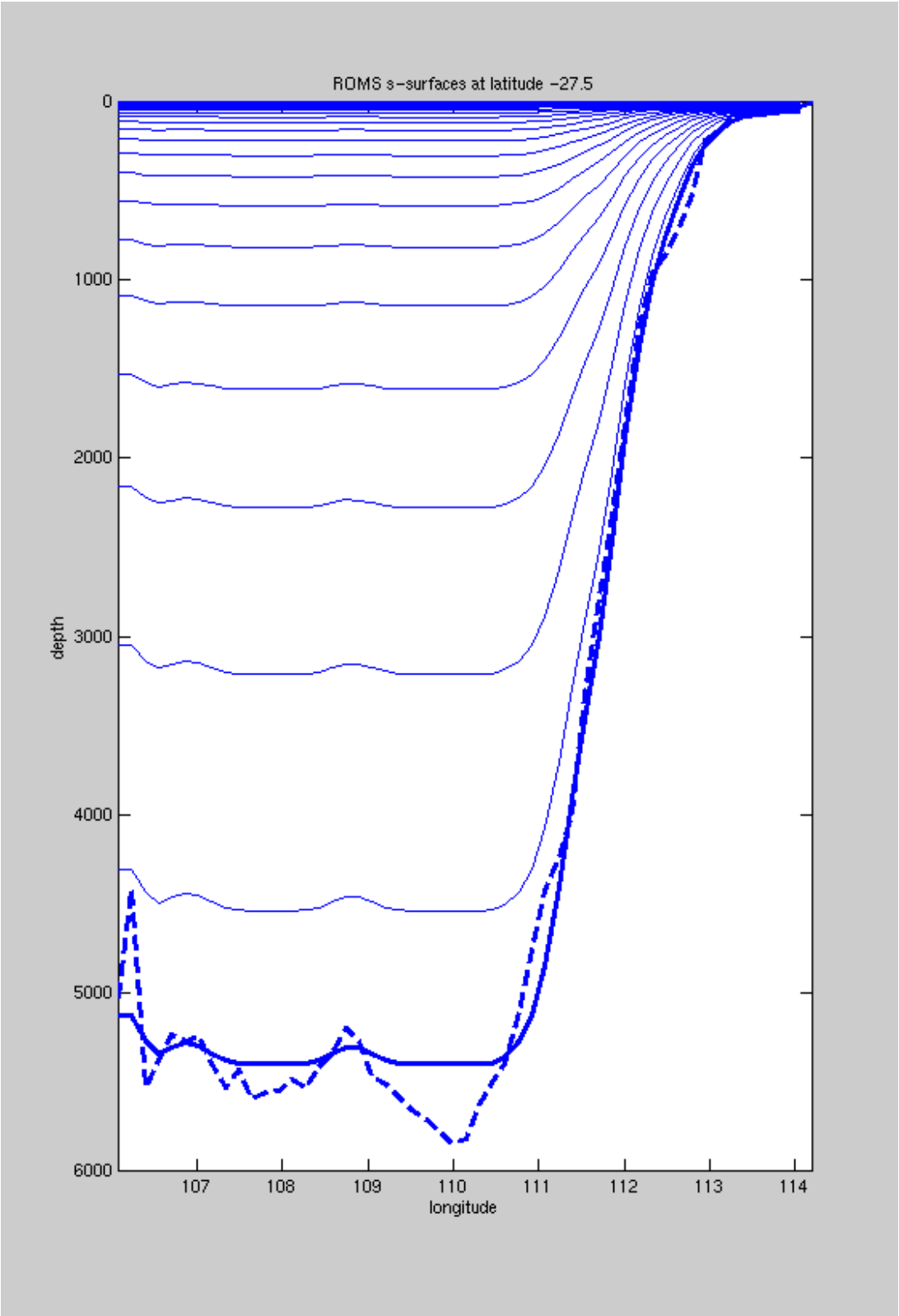

Figure 4 As above, but showing the full water depth along the slice, showing how some of the bottom features are smoothed out.

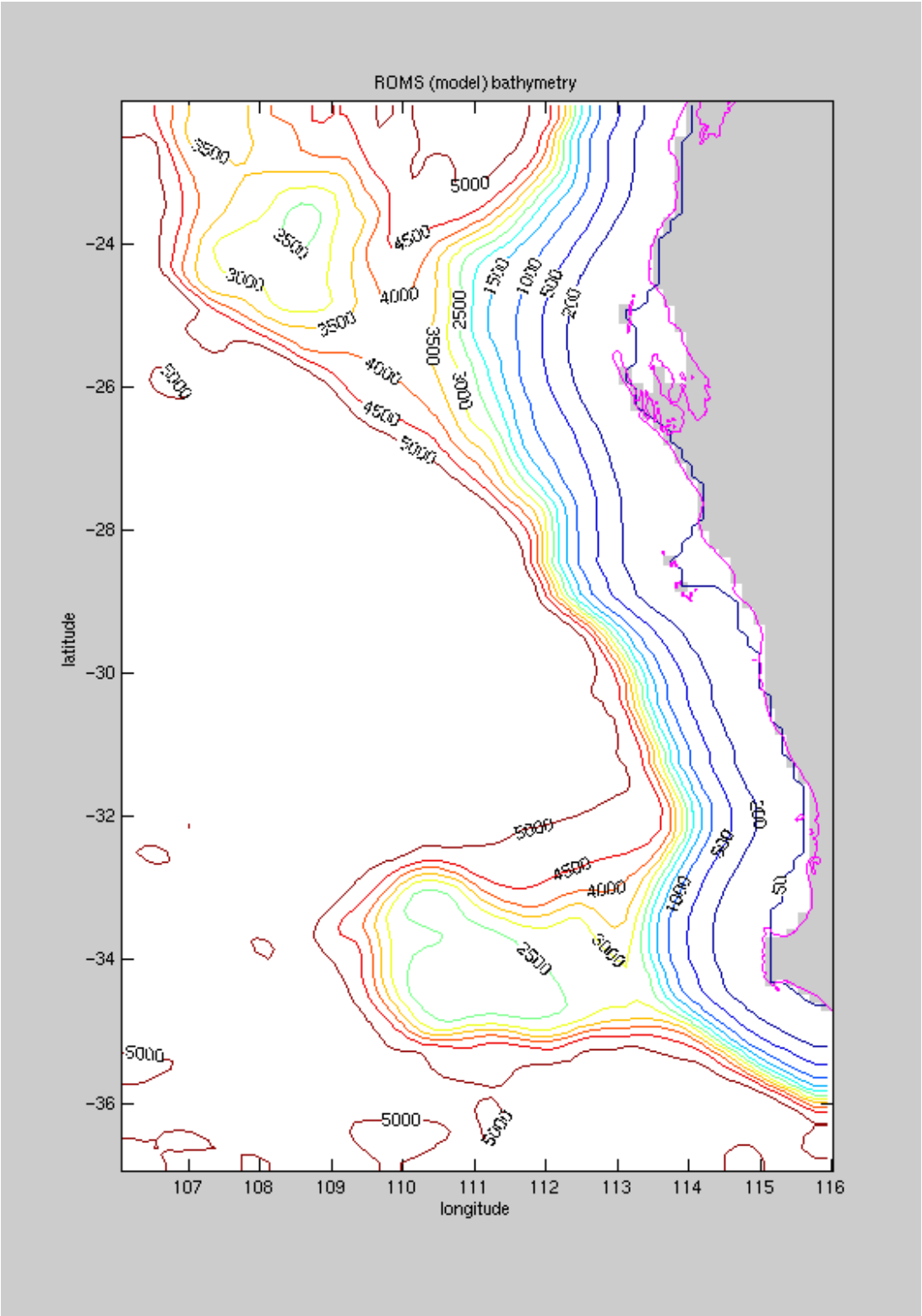

Figure 5 Extent of the model domain, showing the water depth in the model.

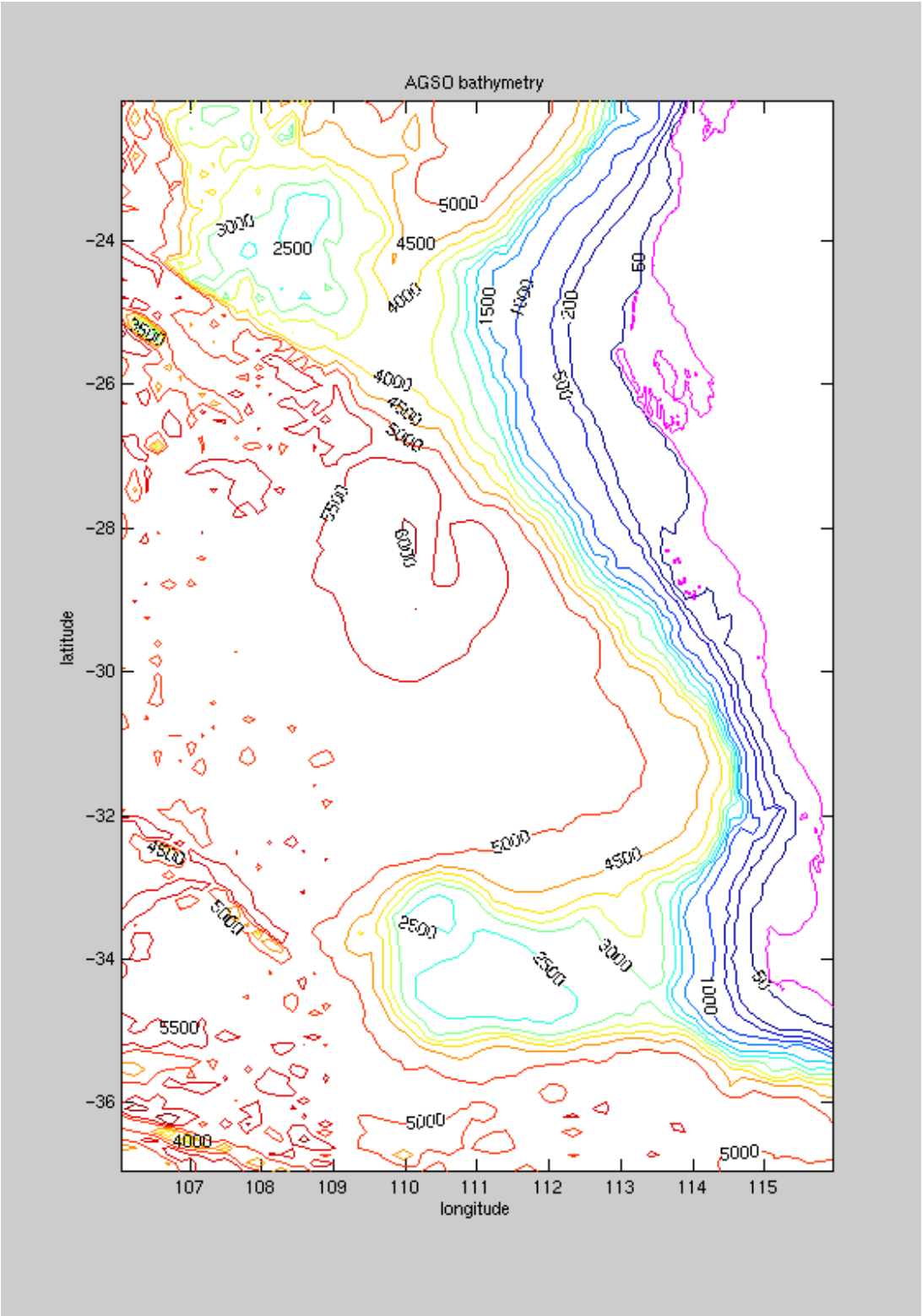

Figure 6 As above, but showing the real bathymetry.

The model is forced at the surface with daily NCEP Reanalysis estimates of the surface wind stress and heat and net freshwater (precipitation-evaporation) fluxes. The problem of specifying initial and lateral boundary conditions for the model, which is usually what limits the performance of hydrodynamic models, is dealt with by the data assimilation scheme.

Data assimilation is the term used in oceanography (and meteorology) for the systematic use of ocean data to improve the accuracy of an ocean model. There is a wide range of methods of data assimilation being developed around the world and it is not at all clear yet which approach will be favoured in 10 years time. A major hurdle at present is that the methods with the most promise are too computationally expensive, by quite a margin, for all but the most powerful computers presently available, for large scale applications. These are the 'variational' methods, and they seek to improve model performance by tracing model errors back to their source and making the required adjustments.

For the present project, however, we have used the much simpler, less costly, but sub-optimal approach known as 'blending' or 'melding', as proposed. The 'melding' method is similar to how weather forecasts are presently made. The cycle starts with an 'analysis', or estimate, of the state of the ocean at some point in time. The ocean model then steps forward in time, with atmospheric forcing and boundary conditions applied. After a certain interval, five days in our case, the model forecast and the next ocean analysis are combined using weights that depend on the error estimates of the data analysis and the model.

To provide the 'analysis' fields, we have used our 'synthetic bathythermograph' or SBT method whereby the satellite estimates of sea level and temperature anomaly are utilised to estimate vertical profiles of both temperature and salinity anomaly. This is done using structure functions obtained by regressing historical measurements of the vertical profile of seasonal temperature anomaly against seasonal anomalies of the surface temperature and dynamic height with respect to a deep reference level. By 'seasonal anomaly', we mean the difference of the observation from the climatological average of that quantity for the location, depth, and time of year. We used the CSIRO Atlas of Regional Seas for the climatology, and also for the climatological relationship of temperature and salinity. The fitting process yielded the error estimates for the temperature and salinity anomaly profiles that are needed for estimating the weights to be used when assimilating the synthetic temperature and salinity profiles into the model.

Results

To document the results of configuring and running the ROMS model for our study area, we have taken the same approach as with the altimetry data and have produced a 2nd CD (see Appendix 5) which comprises movies that can be played on a computer. The movies show temperatures, salinity and water velocity at several depths down to 400m, for 1995 to 1998. Satellite and drifter data are also included for comparison. In the following, we focus more on the issue of the model's suitability to present needs, rather than on interpretation of the model output in terms of oceanography and/or the methodology used.

We have assessed the performance of the model in the same way we tested the performance of the altimetric estimates of near-surface currents – by comparing model estimates with the velocities of drifting buoys, and current measurements by vessel-borne Acoustic Doppler Current Profiler. The results are shown in Fig. 7.

This is the first time that a hydrodynamic model of Australian waters has been run so that its results actually agree, to a significant extent, with *in situ*, virtually un-averaged, observations in the open ocean of the near-surface current. This is a very significant achievement. It is the assimilation of satellite data into the hydrodynamic model that has made this possible.

However, it is apparent that the model does not agree with the *in situ* observations of the surface current any better than do the altimetric estimates derived directly from the satellite data alone. In fact, the model does not agree as well, with the residual r.m.s eastward and northward velocity components being 0.29m/s and 0.27m/s instead of 0.24m/s and 0.23m/s.

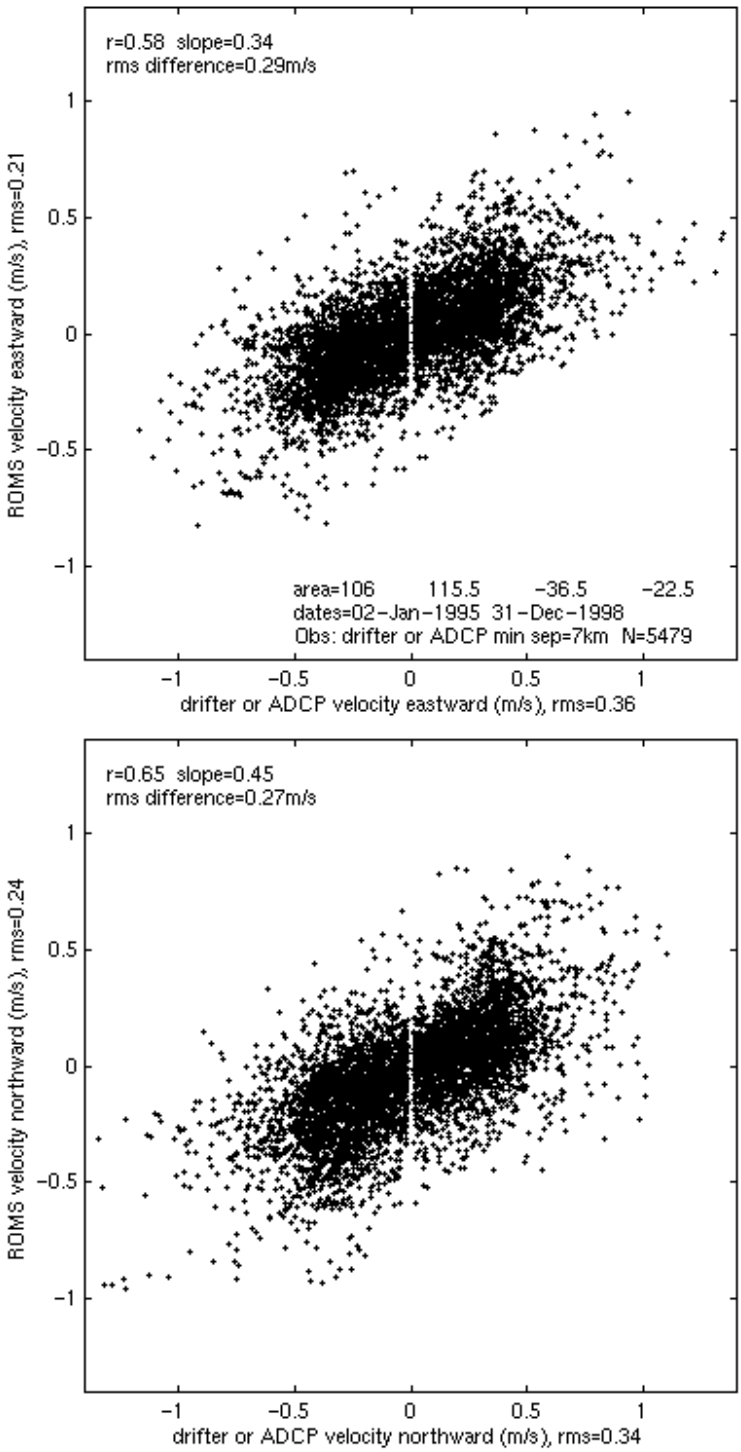

Figure 7 As for Figure 1, but using the ROMS model instead of altimetry.

Many of the model's poorest estimates of the drifter velocities occurred where the model's topography differed most from the real topography. For example, several drifters made rapid orbits around small eddies that were trapped against the continental shelf just off Perth. The existence of these eddies was apparent in both altimetry and thermometry, but because the model bathymetry differed so much from reality, it could not be 'coaxed', by the assimilation of data, to form a type of eddy that belonged in deep, rather than shallow, water. In deeper water, however, the model can also fail to reproduce the correct location of eddies, leading to large velocity errors at the location of drifters. Figure 8 shows an example of the model failing badly to reproduce the observations. The drifter trajectory runs from two days before the panel date to two days after, and shows how the current associated with an elongated cold anomaly transported the drifter right to the shelf break, from 250km offshore, in just four days. The altimetric current agrees with both the satellite image and the drifter trajectory. In the model, however, the cold anomaly bifurcates near the continental slope, with an extension running northwards which is not observed. Also, the warm eddy centred at 31°S 112°E is completely separated from the Leeuwin Current in the model, whereas the observations show the Leeuwin was still feeding into the eddy at that time.

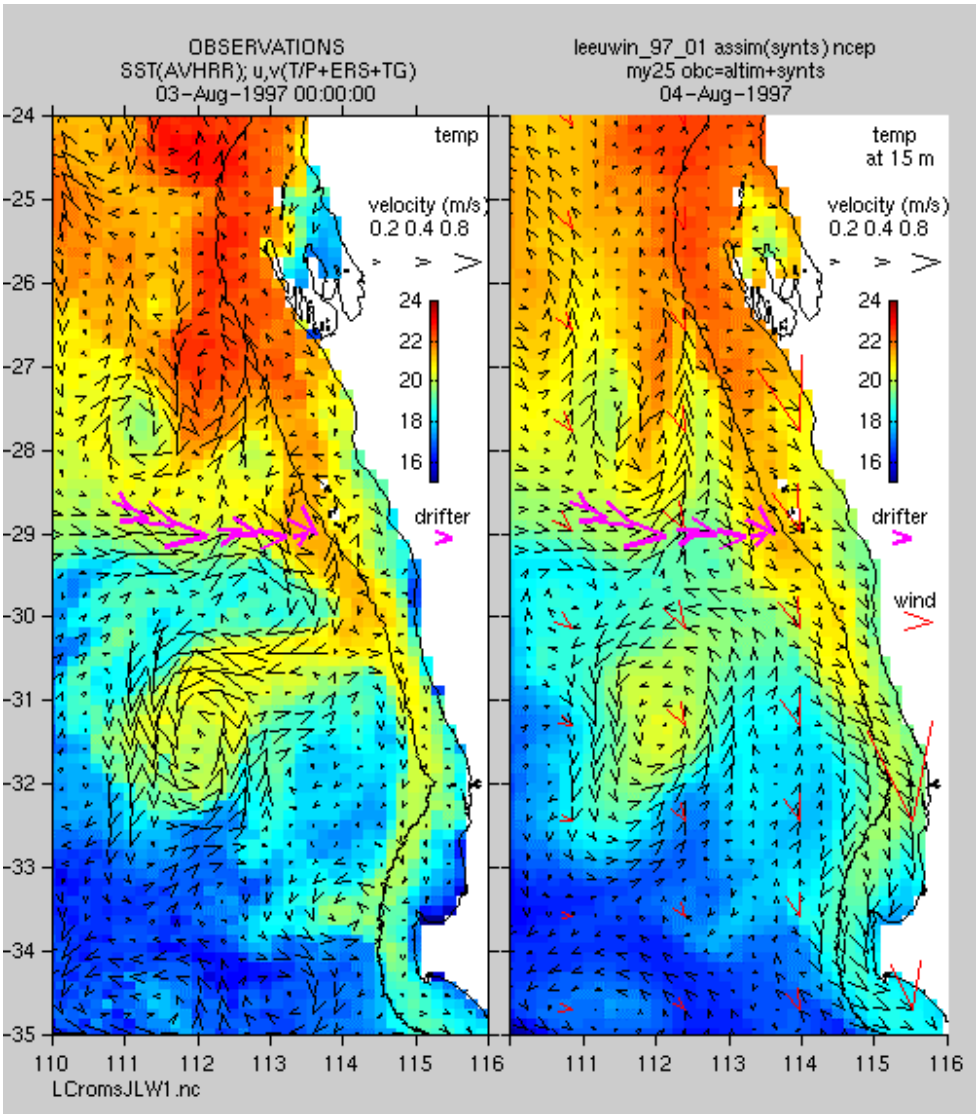

Figure 8 An example of poor model performance. The left panel shows satellite-observed sea surface temperature and altimetric current velocity. The right panel shows the ROMS model hindcast, at 15m depth, for the same time. Both panels show the trajectory of a WOCE drifter that has a sea-anchor at 15m depth.

Figure 9, on the other hand, shows an example of the model succeeding in explaining the trajectory of a drifter *better* than did the altimeter observations. Here, a warm eddy is midway through the process of separating from the Leeuwin Current. The model has the Leeuwin splitting into two streams; one heading offshore to wrap around a cold-core eddy centred at 29°30'S 111°E and the lesser one continuing south to wrap around the warm-core eddy at 30° 15'S 113°. The drifter went offshore in agreement with the model. The altimetric estimate, however, missed the westward stream of the flow, and instead inferred that all the flow of the Leeuwin was continuing south on the offshore side of the warm-core eddy. See Appendix 5 for many more comparisons like these two.

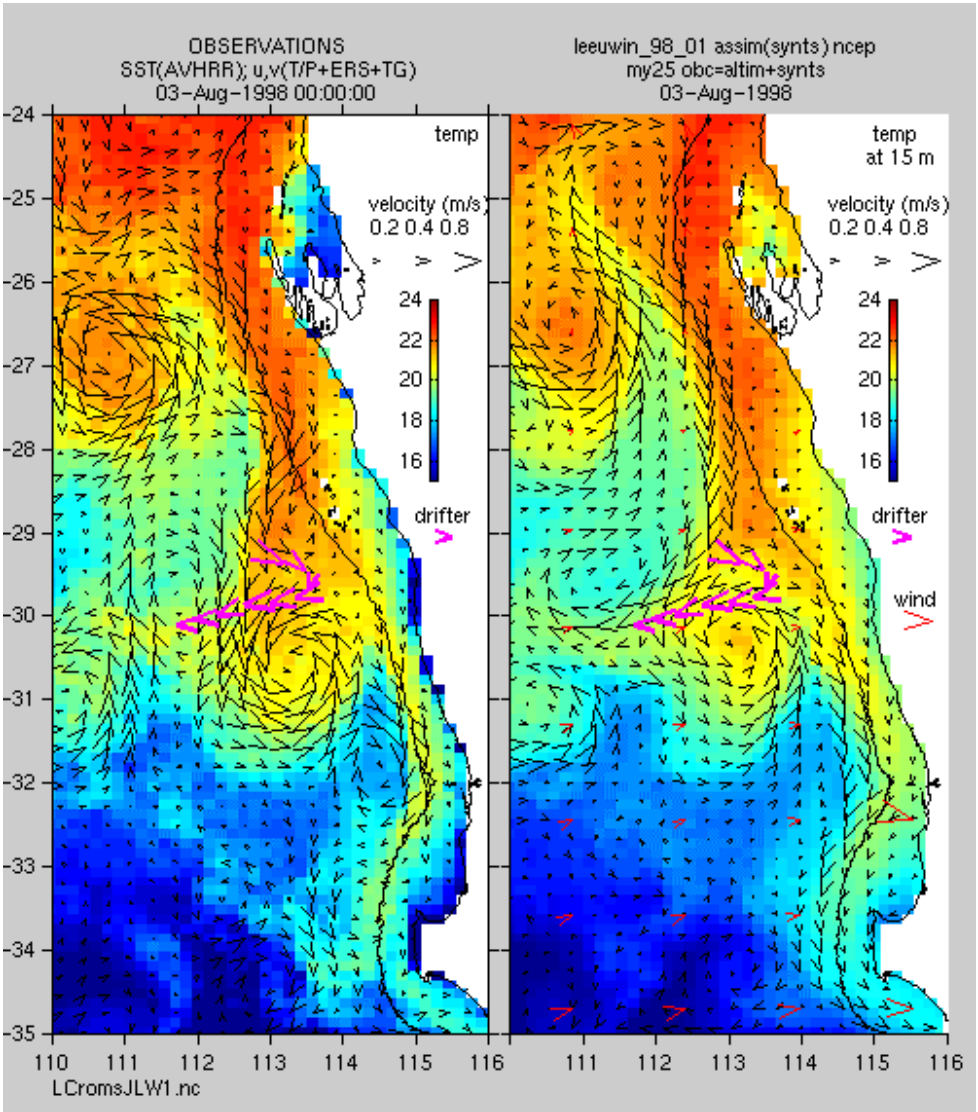

Figure 9 An example of good model performance, indicated by the fact that the model agrees with the drifter better than the altimetric velocity map does.

It is harder to know whether the model is adding value to the satellite-derived, three-dimensional, temperature and salinity fields assimilated into it, because very few, especially of salinity, *in situ* sub-surface observations were made in the region in the years for which we have all the data required for running the model.

Figure 10 shows a comparison of the vertical profiles of r.m.s differences from *in situ* observations (made by expendable bathythermograph, or XBT) of 1) the CARS climatology, 2) the satellite derived 'synthetic bathythermograph' (SBT) and 3) the result of assimilating the SBT into ROMS.

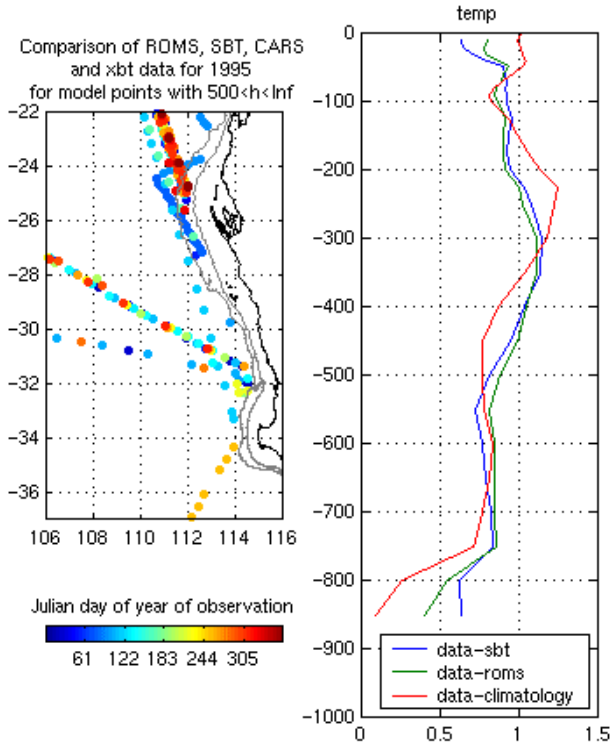

Figure 10 Comparison of *in situ* temperature profiles (obtained by expendable BathyThermograph) with three hindcasts. The left panel shows the locations of the XBT drops, coloured to indicate the day of year of observation. The right panel shows the vertical profile of the rms error of three hindcasts of the observations. The first hindcast uses just the CARS seasonal climatology. The second augments this with satellite observations of surface temperature and height anomaly, processed to produce Synthetic BathyThermographs (SBT). The third is the result of assimilating the SBT estimates into the ROMS model.

Near the surface, the SBT agrees best with the XBT observations, probably because satellite estimates of SST are used in forming the SBT. The model error was greater but still less than the CARS climatology. From 100 to 300 m depth, the model is marginally more skillful that the SBT analysis or climatology. This is the depth range where thermal anomalies are most strongly correlated with sea level variability, and indicates that the model is exhibiting the capability to improve upon the data analysis alone. At greater than 300 m depth, however, it appears that neither the SBT nor the model are appreciably

better than simply using climatology. Similar results (not shown) are obtained for 1996, and for when CTD data is used instead of XBT. This is disappointing, considering that the SBT method works very well off eastern Australia. In this depth range the estimated error in the SBT analysis was only slightly less that at shallower depths, and hence the model has not departed appreciably from the analysis. It is clear that improvements to the performance of the SBT method will have to be made for it to be a useful way of assimilating the altimeter data into models off southern Western Australia. We suspect that the very complex spatial variability of the T-S relationship in that region is the reason for the poor performance. The sparcity of *in situ* observations, however, obliges us to bin the data over a wide region. Previous physical oceanographic field studies in the Leeuwin Current have revealed that the 300 m depth level commonly marks the depth at which southward surface flow reverses to northward Leeuwin Undercurrent flow. The independence of the deep and shallow currents will prove a limiting factor for data assimilation modeling in the region, until subsurface observations become available to augment the data analysis. The recent advent of the ARGO global array of profiling floats provides a cost-effective means of acquiring these data. The first few ARGO floats have recently been deployed off NW Australia by CSIRO

Discussion

For this project, we proposed two methods of hindcasting, for a selection of recent years, what the ocean currents were doing off Western Australia, in order to examine the role of advection in the early life history of western rock lobster and other Western Australia commercial species. The first method was to estimate the surface currents directly from satellite data using a simple, steady-state dynamical equation that relates gradients of sea level to surface velocity. In the second method, the satellite observations are essentially 'filtered' by feeding them into a fully non-linear hydrodynamic model. The assumption here was that the model equations constitute information about the way the ocean evolves from one state to another, so the model should be able to function as the optimal interpolator. The modeling step was envisaged to be necessary because the altimeter data were assumed to be both too sparse, and too highly contaminated with measurement error to be of use directly, at the length-scales and time-scales of interest.

It has turned out, however, that the altimetric surface current estimates are better than anticipated, and that the model is not able to improve upon them. The most likely explanation for this outcome is that the amount of 'misinformation' added during the modelling step must outweigh the benefit of using the full dynamic equations to interpret the satellite data. The two major sources of misinformation we have identified are 1) errors in topography that were made to keep computational demands reasonable with today's computers, and 2) errors made in translating the altimetric estimates of surface elevation into a form (profiles of temperature and salinity) suitable for assimilation to the model with established, but sub-optimal, methods of data assimilation.

It must also be recognized that the sub-optimal 'melding' scheme for assimilating data utilizes data analyses that are significantly smoothed in the optimal interpolation gridding step. There is, therefore, a loss of information at short time and length scales in the analysis step, prior to incorporation in the model. The direct assimilation of observations

on a point by point, time by time basis, according to when and where the data were observed, would retain short scales in the data and accordingly allow the model the opportunity of evolving these features in the simulation. The aforementioned 'variational' data assimilation methods, presently being implemented in the most recent version of the ROMS model, are designed to utilize the data directly to this end.

The good performance of the altimetric current analyses was recognized early in the project and a decision was made to rely, at least initially, on that method for meeting the requirements of the application to larval advection. This is why the extra time was spent refining the method, for example, to extend coverage shorewards right to the coast. That decision appears now to have been the right one, since the work to develop the model to the point where it is worth using for larval transport simulations will have to done as part of a subsequent project.

Larval advection model

Methods

Larval advection models can be either Eulerian, like that of Chiswell and Booth (1999) or Lagrangian, like those of Polovina *et al*. (1999) and Incze and Naimie (2000), who modelled, respectively, transport of the larvae of *Jasus edwardsii*, *Panulirus marginatus* and *Homarus americanus*. We have chosen the Lagrangian (or individual-based) method, wherein the positions of individual model larvae are advanced at regular intervals (8 h in our case) by a displacement that depends on an estimate of the water-velocity field at the depth and location of each larva at each time. Larvae make diel vertical migrations, according to their age, but do not swim horizontally. The displacement of pueruli, however, includes swimming. We used a 4th-order Runge-Kutta integration scheme (Hofmann *et al*. 1991) to ensure that model larvae did not diverge from regions of circular flow.

Hatching

Mature *P. cygnus* begin to mate in late autumn and the first-stage larvae hatch throughout the summer from November to February with a peak in January (Chubb 1991). Incubation is faster at higher temperature (Aldrich, 1967); most females produce two broods per season (Chubb, 1991).

We modeled the hatching of larvae by releasing a constant number of model larvae every five days from 1 November to 28 February at a line of locations along the outer continental shelf of Western Australia between latitudes 27°S and 34° 20'S, where adults are concentrated.

Vertical migration

Vertical migration behaviour of *P. cygnus* larvae is well known due to extensive field sampling (Ritz 1972; Phillips *et al.* 1978; Rimmer and Phillips 1979; Rimmer 1980; Phillips and Pearce 1997), although the controlling factors are unknown. All larval stages avoid light, and are principally found near the surface at night and at depth between sunrise and sunset. The later stages make greater diurnal migrations than the early stages, and only come to the surface on the darkest of nights, and then only if winds are relatively weak.

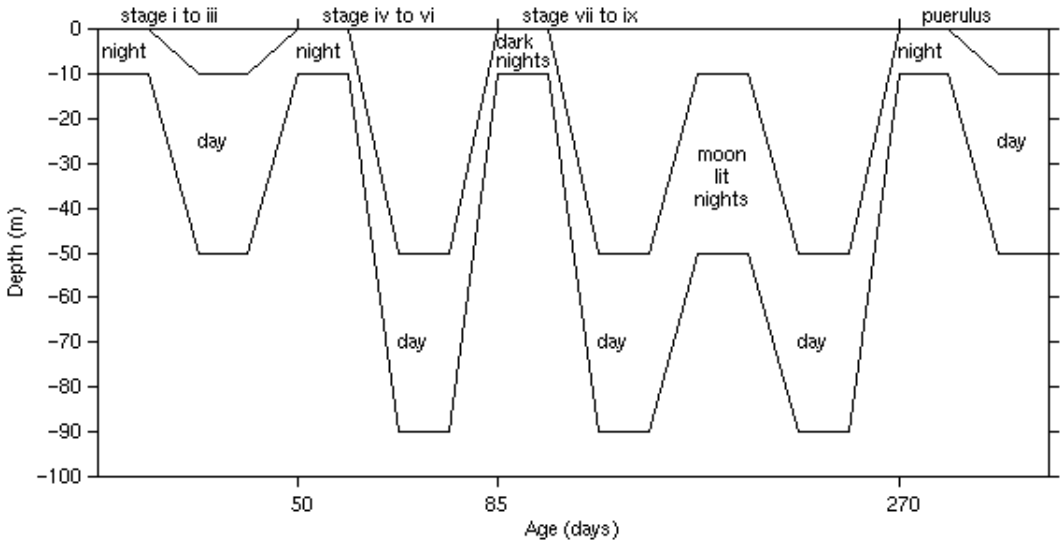

Figure 11 Schematic of the model depth strata occupied by model larvae by night and day as a function of larval age

We modeled vertical migration (see Fig. 11) by dividing observed behaviours into three classes. Model larvae graduated from one class to the next as they reached critical ages. In the vertical dimension, we discriminated three depth strata: upper (0-10m), mid-depth (10-50m) and deep (50-90m). Early-stage (I-III, ages 0-50d) larvae were in the upper layer at night (2100-0500; one model time-step) and the middle layer by day (0500-2100; two model time steps). Mid-stage (IV-VI, ages 50-85d) larvae descended to the deep layer by day. Late-stage (VII-IX, ages 85+d) ascended to the surface layer only within three days either side of a new moon, otherwise they ascended to the middle layer.

The puerulus stage

Much less is known about the puerulus stage than larval stages, as there have been few pueruli collected in plankton tows (Phillips and Pearce1997). Pueruli are strong swimmers (Phillips and Olsen, 1975) and do not feed (Lemmens, 1994), suggesting that they are rarely sampled because they spend a short time as pueruli. In the laboratory, the swimming puerulus phase lasted only a week or so (Lemmens 1994). Pueruli are caught in coastal collectors almost exclusively within two days of the new moon (Phillips, 1975).

To compare our simulation results with observed puerulus settlement rates, we modeled the puerulus stage, despite uncertainty over triggers of metamorphosis, depth strata occupied by the puerulus, their swimming speed and duration, and settlement habitats. We used two metamorphosis scenarios: one where all larvae metamorphosed as soon as they reached an age of 270 days, and one where metamorphosis occurred when larvae of age greater than 270 days first encountered the continental slope (depth < 2000 m) within three days of new moon. Once metamorphosed, model pueruli swam eastwards at $\mathbf{v}_{swim} = 0.1$ m/s plus the current velocity in the surface layer at night and in the middle layer by day. If they reached water shallower than 100 m within three days of new moon, they were counted as settling successfully. If currents carried them offshore, they were given one more month to settle, although it is doubtful this occurs in reality. Our modeling of the puerulus stage was a weakness, and the number settling in the model should be interpreted as an index of the number of late-stage larvae encountering the continental slope near new moon. The observed settlement rates exhibited a high degree of spatial and within-year correlation, however, so we suspect that *variability* of puerulus mortality may not be very high, in which case our approach is justified. Further, Caputi *et al.* (1996) and Caputi *et al.* (2001) showed that there is a substantial lag in the correlation of larval settlement rates and environmental variables, suggesting that conditions at the time of metamorphosis and settlement do not drive settlement variability.

Velocity fields

Estimates of the current velocity for advecting the larvae were not, for the work reported here, obtained from our ROMS hydrodynamic model of the region, but from altimetry, for the reasons discussed above. However, $\mathbf{v}_{altim}$ is incomplete as an estimate of the total current because 1) it is not possible to estimate the time-mean of the sea level field accurately at a high spatial resolution, so the mean was removed, 2) wind-driven motions can not be diagnosed directly from sea level, and 3) small-scale and very transient non-wind-driven currents are not adequately resolved using the two existing (nadir-only viewing) altimeters.

Our larval advection model required estimates of the depth-averaged current $\mathbf{v}_1, \mathbf{v}_2$ and $\mathbf{v}_3$ within 0-10 m, 10-50 m and 50-90 m. We estimated these by augmenting the altimetric estimate differently for each layer as follows:

$$\mathbf{v}_1 = \mathbf{v}_{m1} + \mathbf{v}_{altim} + \mathbf{v}_{Ek} + \mathbf{v}_{sfc} + \mathbf{v}_{rand} \quad (4)$$

$$\mathbf{v}_2 = \mathbf{v}_{m2} + \mathbf{v}_{altim} + \mathbf{v}_{Ek} + \mathbf{v}_{rand} \quad (5)$$

$$\mathbf{v}_3 = \mathbf{v}_{m3} + a\mathbf{v}_{altim} + \mathbf{v}_{rand} \quad (6)$$

For the deepest layer (see (6)), we attenuated $\mathbf{v}_{altim}$ by a= 0.8, which is the average observed attenuation, at that depth, of anomalies of dynamic height in the study region.

Open-ocean, wind-forced velocities $\mathbf{v}_{sfc}$ *and* $\mathbf{v}_{Ek}$

The effect of wind stress could straightforwardly be incorporated into (4) and (5), except that there was a mismatch of the time and length-scales of the sea level and wind stress data available to us, which reflected the spectra of the ocean and atmosphere, respectively. We approximated the total velocity in the upper-two layers as the sum of a (slowly varying) component primarily associated with pressure gradients, and (more rapidly varying, but more spatially coherent) components associated with local wind forcing. We estimated the surface wind drift $\mathbf{v}_{sfc}$ as being 3.5% of the wind at 10 m height, rotated 20° left (eg: Katz *et al.*, 1994). Estimates of the 10 m wind at 12 h intervals were those of the NCEP-NCAR 40-year reanalysis on a 1.9° by 1.9° grid (Kalnay *et al.*, 1996). These analyzed wind estimates compared well with observed winds at Fremantle, although the strength of the diurnally-varying sea breeze component was under-estimated by about a half. We did not compare them with *in situ* observations offshore.

To estimate the time-dependent velocity $\mathbf{v}_{Ek}$ of an Ekman layer of constant thickness 50m, we used the simple Pollard and Millard (1970) method, which simulates the damped inertial oscillations resulting from transient wind forcing. The model was forced with the NCEP-NCAR daily-averaged wind stress and we used a linear interfacial friction coefficient of 0.002m/s.

Time-mean velocities $\mathbf{v}_{m1}, \mathbf{v}_{m2}$ *and* $\mathbf{v}_{m3}$

Finally, estimates of the geostrophic (i.e., excluding the wind-driven component) mean velocity fields for 1993-1998 were required for the three model strata. For many regions, the climatological-average dynamic height fields estimated from historical hydrographic data serve this purpose. The present study region, however, has not been surveyed very intensively and the value of the existing data for estimating the mean state was reduced because of the large amplitude of the transient eddy field. For all study regions, there were also the problems of selecting a level of no motion, and computing the height field over the continental slope. The best available estimate of the mean dynamic height field was that of the CSIRO Atlas of Regional Seas (CARS). We used this to estimate the mean velocities $\mathbf{v}_{1m}, \mathbf{v}_{2m}$ and $\mathbf{v}_{3m}$ at 0 m, 30 m and 75 m depth, respectively, assuming a level of no motion at 300 m. Since it is unclear that 300 m is indeed the best choice of a level of no motion, we assessed the impact of this choice by also computing the flows with respect to 1000 m and 2000 m.

Another estimate of the three-dimensional time-mean velocity field was derived from a new global ocean model ACOM3 recently developed at CSIRO. This is essentially a finer-resolution (1/3° latitude by 1/2° longitude) version of the model of Schiller *et al.* (2000), forced by 3-day averaged NCEP-NCAR and FSU atmospheric fluxes. We estimated the sub-Ekman layer mean velocity field for our model depth strata by averaging the ACOM3 estimates of the flow fields for 1992 to 1998 between 30 m and 60 m and 60 m and 100 m. We did not use the ACOM3 Ekman layer response (either the mean or the transients) because it was not straightforward to separate it from the pressure gradient-associated flows, which we estimated by altimetry and did not want to double-count.

Unresolved random velocities $\mathbf{v}_{rand}$

Our comparison (Fig. 1) of $\mathbf{v}_2$ with drifter velocities showed that the unresolved variance of the observations had a root-mean-square value of about 0.2 m/s. Some of these errors were associated with failure of our model to represent sharp frontal features, but much was due to an absence of small–scale turbulence. Hence the need for additional random velocities $\mathbf{v}_{rand}$ in (4)…(6) to bring the total modeled velocity variance closer to that of the observations. As a first step towards correctly simulating the error covariance time- and length-scales, we added independent random velocities of root mean squared amplitude 0.05 m/s to the altimetric velocity grid (20 km, 5 days), and 0.1 m/s at the individual tracked-particle level (any separation, every 8 h).

Year classes modeled

We simulated the fate of six year classes following the launch of Topex/Poseidon. The first of these year classes, which resulted from hatchings over the 1992-1993 summer, was the 1993 year class. The last was the 1998 year-class, whose tail end of modeled settlement was missing since we had not yet processed all data streams for 1999.

Results

The complete larval advection model has more than 20 important parameters. We discuss here first the intra- and inter-annual results of a model run that used the parameter values discussed above and the mean field of the global circulation model. Next, we discuss the impact of varying those parameters on model results.

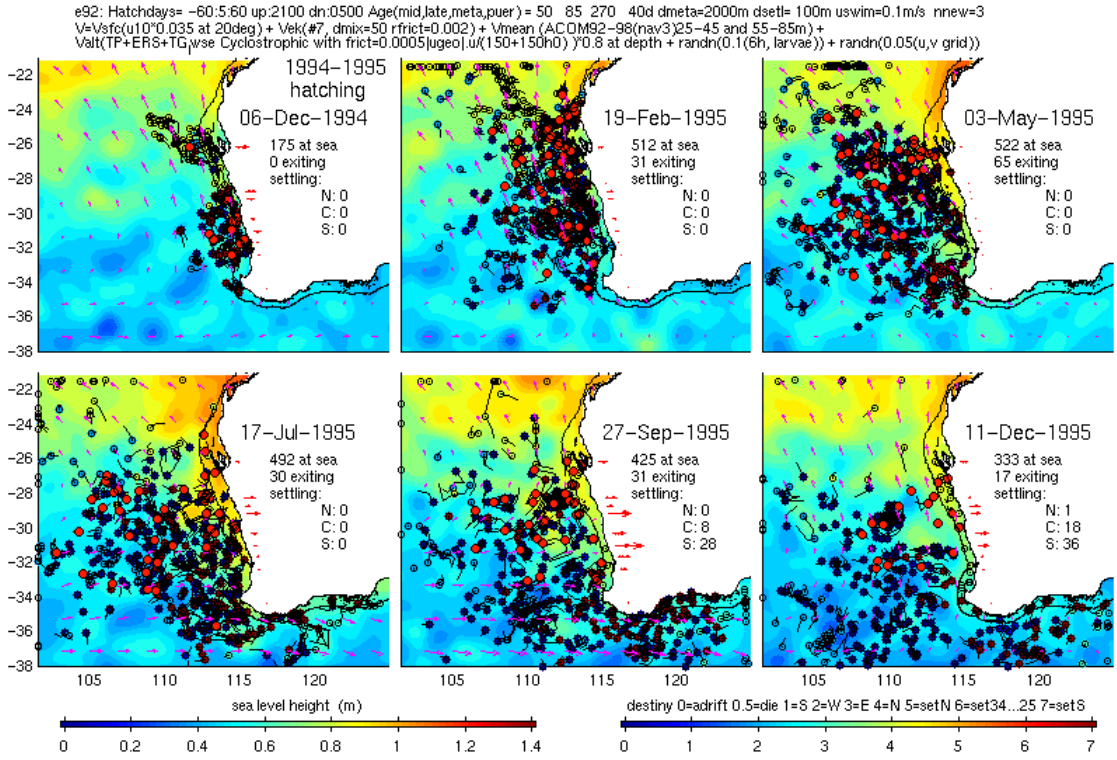

Figure 12 Modeled fate of the 1995 year-class. The positions of model larvae are shown at 73-day intervals, from 30 days after the first larvae are released, to one year later. Tails indicate trajectories over the previous five days. Larvae are colour-coded by their eventual destiny, red indicating the individuals that subsequently 'settle' (see text) within the fishery (34° S-25° S). The number of these, as well as how many settle north (N:) and south (S:) of the fishery, is shown in each panel along with the number still at sea and the number exiting since the previous panel. Positions at which larvae exited are marked with open circles. The background colour field shows the interval-averaged altimetric sea level height anomaly about the 1993-1998 mean, plus the climatological surface dynamic height with respect to 300m. Magenta arrows show the interval-averaged NCEP-NCAR wind stress. Red arrows on the land at the latitudes of coastal collectors indicate the observed rates of puerulus settlement. Model parameters are listed along the top.

A sequence of snapshots of the positions of model larvae for the 1995 year-class is shown in Fig. 12. Appendix 4 includes an animation of the positions of larvae from hatching to settling, for all six year-classes simulated. The striking feature of this simulation is that most of the model larvae remained within the latitudinal range of the adults, at least by the beginning of May. Most of the early-stage larvae leaving the model domain by May did so to the north or west. The northwestward influence of the strong summer southerly winds was largely, but not completely, countered by the eastward and southward influence of the geostrophic current. Model larvae taken north of 23°S had little chance of returning.

The distribution of model larvae in July was broadly consistent with the June-July distribution observed by Phillips (1981).

By September, the balance had shifted as the winds south of 30°S had swung around to westerlies, the south-easterlies north of 30°S had weakened, the Leeuwin Current had passed through its period of maximum flow, and larvae were at greater depth. Many model larvae rounded Cape Leeuwin by September. Very few returned. This result appears unlikely since puerulus settlement is minimal at Cape Mentelle. The greatest observed settlement at Cape Mentelle, however, was in years of strong Leeuwin Current.

In addition to a general northwards then southwards oscillation, a westward spread of the model larvae with time occurred, which was not simply due to the wind. The velocities associated with the mesoscale eddy field were typically 10 times those of the mean geostrophic field or wind. Consequently, larvae were constantly changing relative position within the population. The distribution, at any instant, of the individuals destined to 'settle' (shown in red) was patchy but essentially random throughout the range (23°S-35°S) of the population.

The offshore extent (see Fig. 13) of larvae that eventually settled was less distinct. Some model larvae returned from as far west as 105°E, a distance of more than 1000 km, but many more achieved only 600 km.

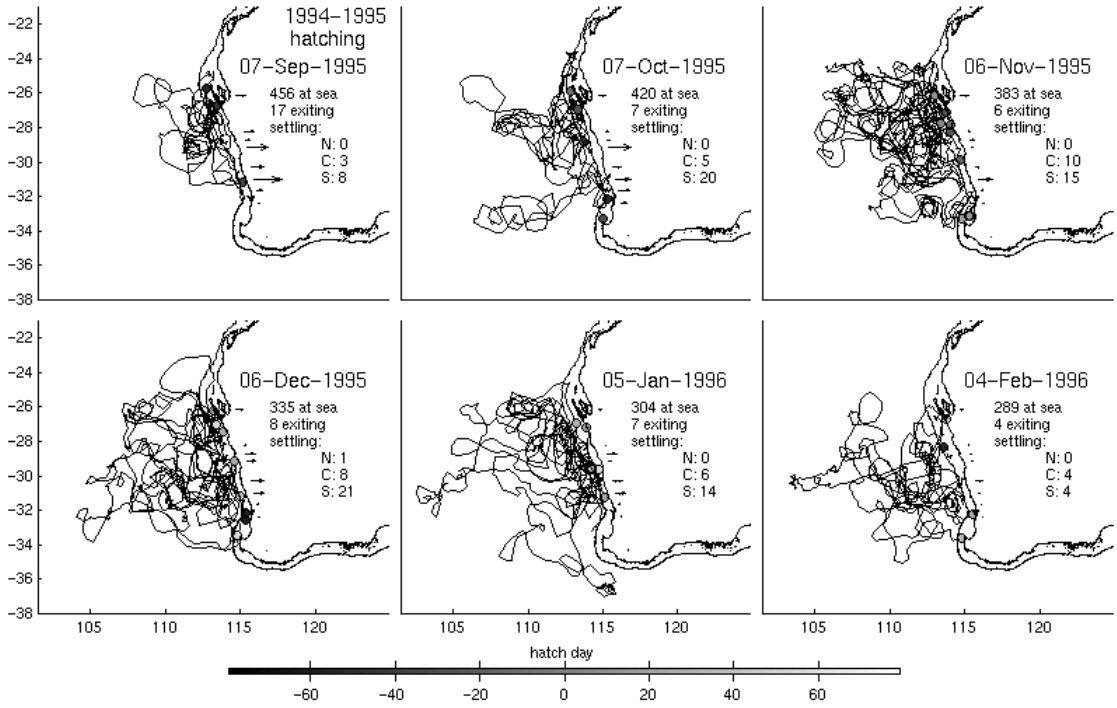

Figure 13 Trajectories of those model larvae that return to the fishery. Each panel shows the complete trajectory from hatching to settlement of just those larvae settling in the central region (34° S-25° S) during the month prior to the panel date. The arrival point on the shelf is shown as a circle shaded to indicate the hatch day (0=1 January) of the larva. Arrows on the land at the latitudes of coastal collectors indicate the observed rates of puerulus settlement during the same period

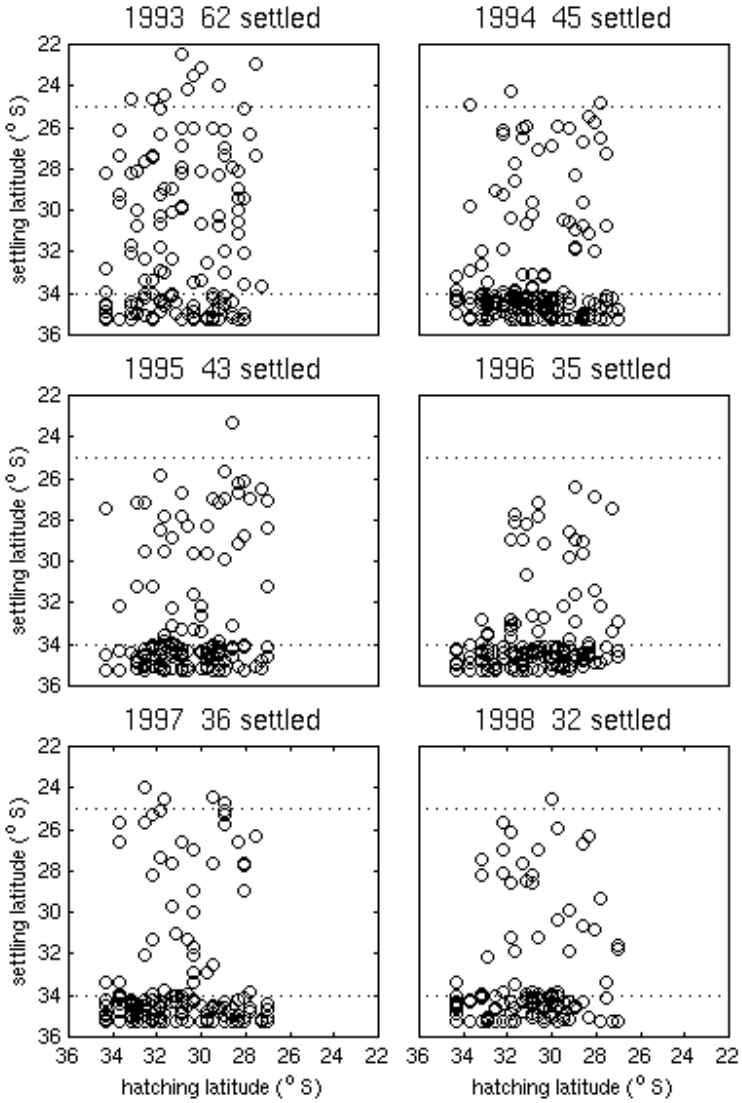

Figure 14 Settling latitude versus hatching latitude of individual model larvae. The total number settling (of 625 released) within the fishery (between 34°S and 25° S, and west of 117° E) is shown for each year.

One consequence of the vigorous mixing by the eddy field was that the probability of eventually settling was independent of hatching latitude (see Fig. 14). That this was a consequence of the mixing by meso-scale eddy field was demonstrated by experimentally setting the altimetric velocities to zero in the model (see Fig. 15). Note how the red, eventually-settling model larvae were tightly clustered in that case. Despite the clustering and a shoreward jet near the Abrolhos Islands, they did not settle within the same area; settlement remained broadly distributed.

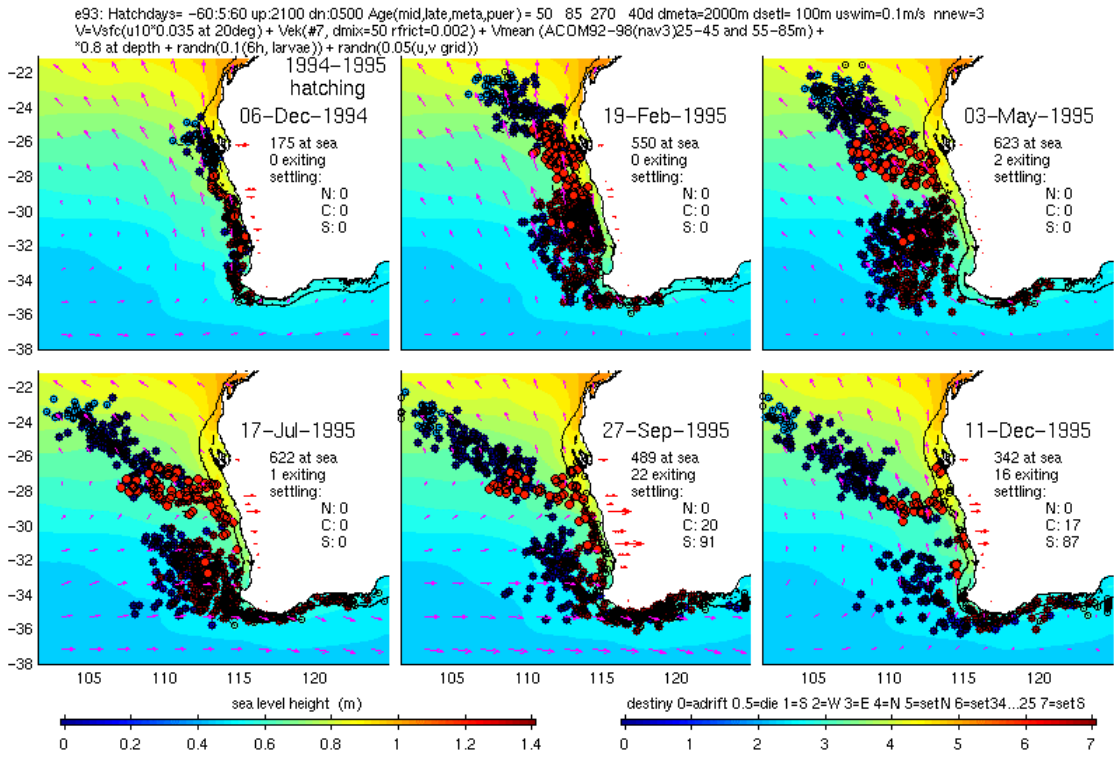

Figure 15 Results of the model run with the altimetric velocity set to zero, leaving only the mean, wind-driven and random velocity components. The climatological mean surface dynamic height with respect to 300m is shown.

For this model run with no mixing by eddies, settled individuals were mostly hatched near the Abrolhos Islands (Fig. 16), suggesting that, were it not for mixing by eddies, the Abrolhos Islands would be the optimal spawning location. No experiments resulted in hatching date being important.

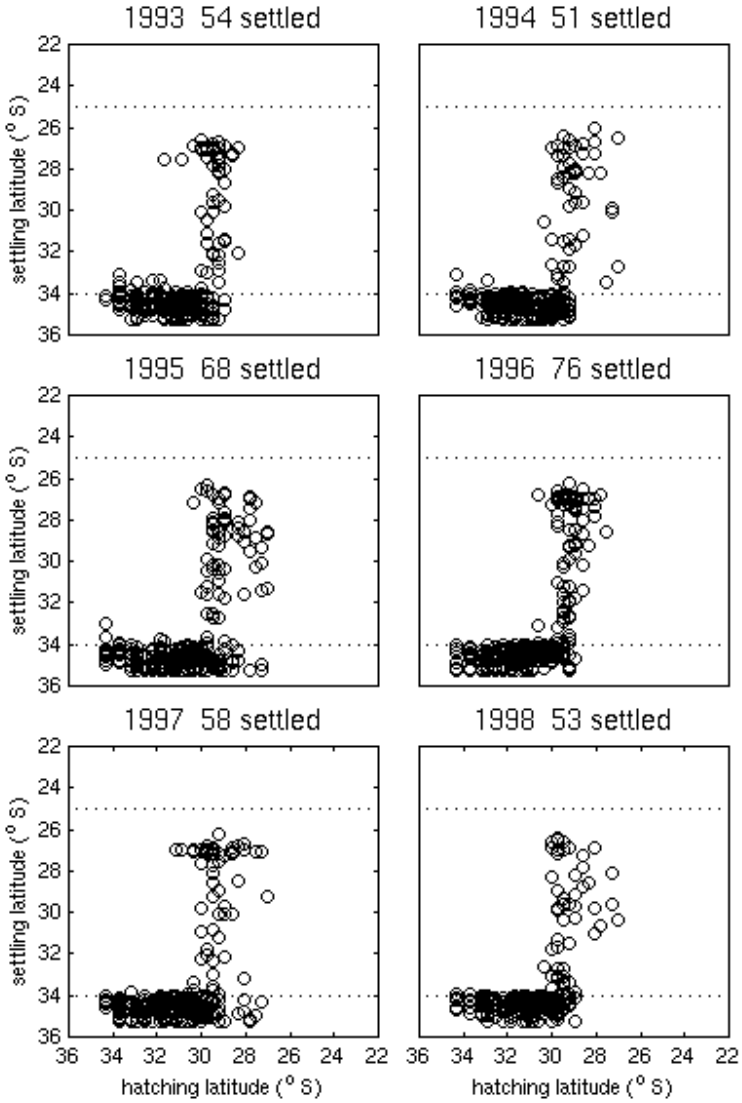

Figure 16 Settlement latitude-hatching latitude relationship when the altimetric velocity is set to zero in the model.

While eddies were responsible for mixing at one length-scale, it also appeared that they are agents of anti-diffusion at a smaller scale. Inclusion of the small amount of interfacial drag in (1) and (2) was enough to make the surface field sufficiently convergent for model larvae to be significantly associated with cyclonic eddies, rather than with anti-cyclonic eddies. If this occurs in nature, it could have a significant impact on larval mortality, since the prey field is potentially very different between the two eddy environments. Inspection of SeaWiFS chlorophyll-a estimates for 1997-1999 (see Appendix 4 and Fig. 17) showed that cyclonic eddies had no surface expression in chlorophyll-a, while the anti-cyclonic eddies of shelf waters shed by the Leeuwin were higher in chlorophyll-a. It may be, however, that cyclonic eddies have significant productivity at depth which is not detected by satellite (Millan-Nunez *et al.*, 1997).

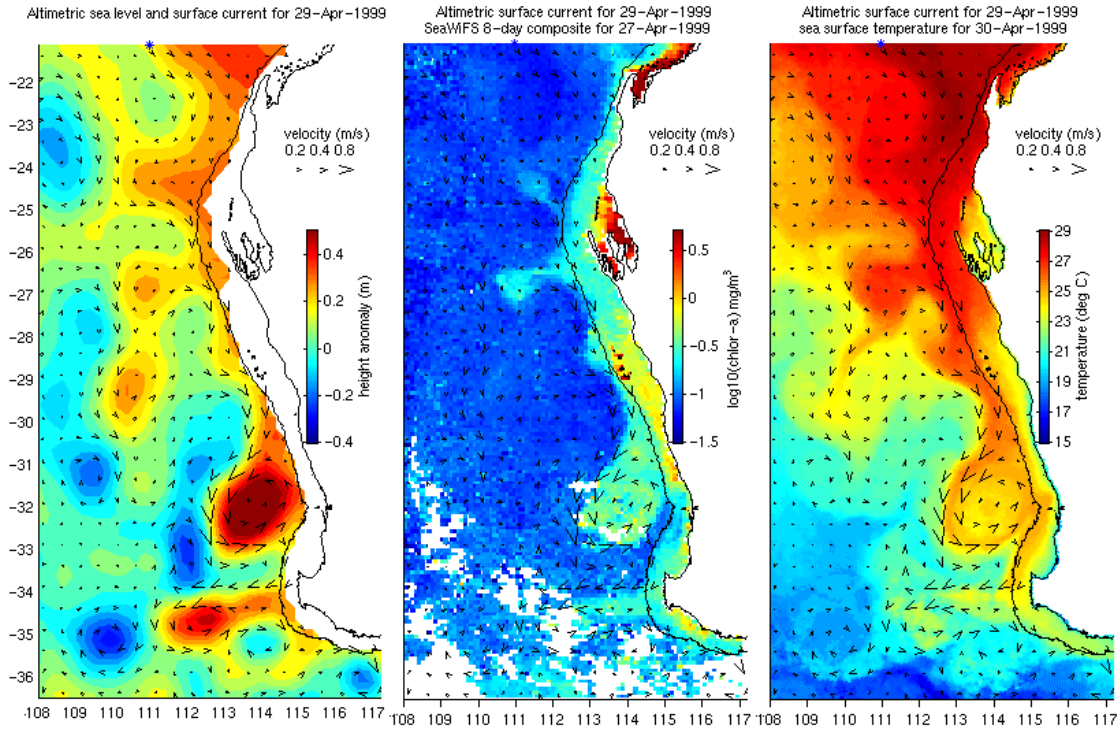

Figure 17 Maps of the study region comparing *i)* the sea level height anomaly measured by satellite altimeters, *ii)* chlorophyll-a concentration measured by SeaWiFS imagery of ocean colour, and *iii)* sea surface temperature measured by NOAA satellite AVHRR thermal imagery. Arrow heads in all panels show the geostrophic surface current inferred from the sea level field. The 200m isobath is shown.

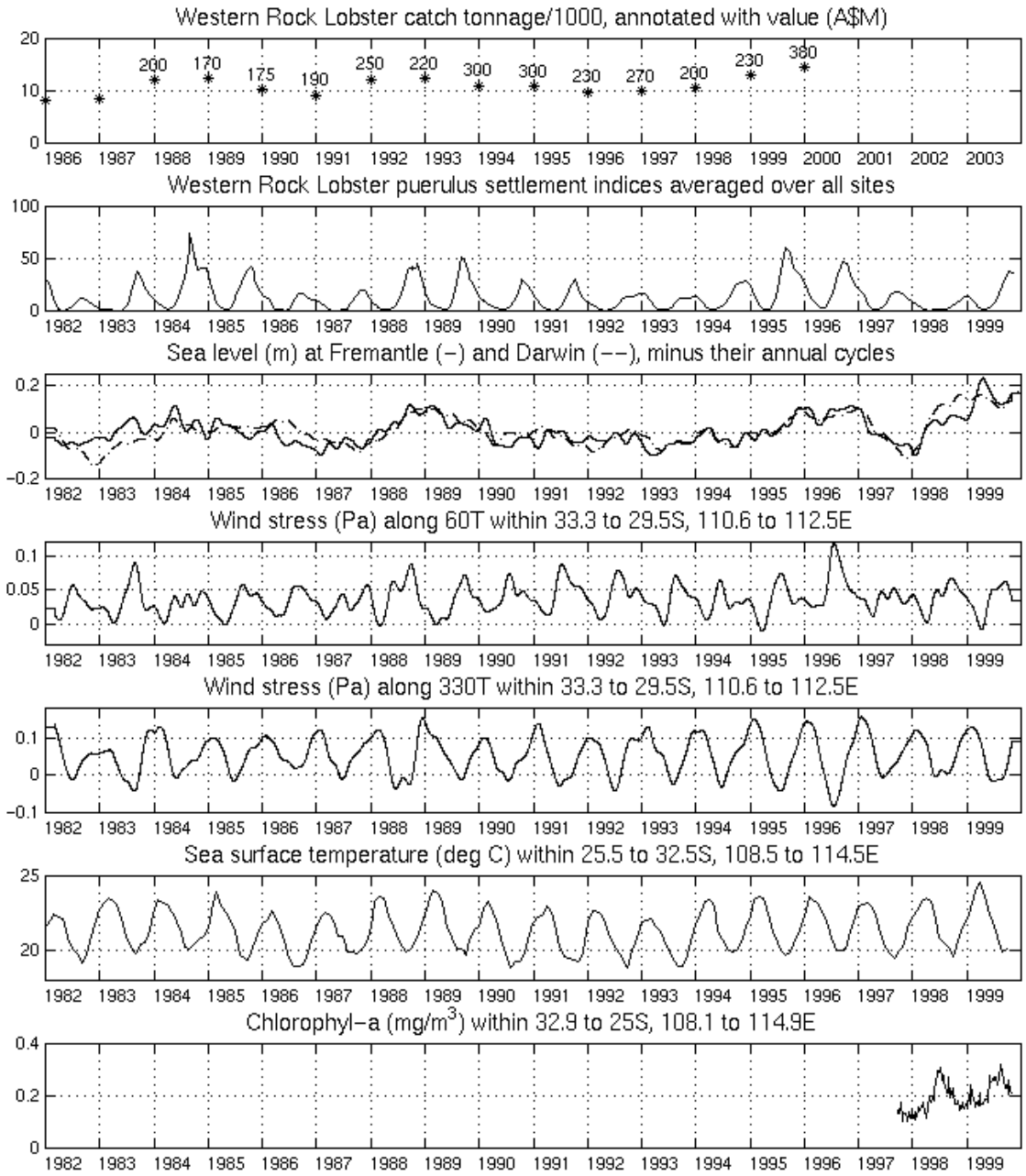

Figure 18 Time series of *i)* annual tonnage and value of commercial catches of *P. Cygnus*, *ii)* monthly puerulus settlement indices averaged over all monitoring sites, *iii)* 60-day averaged sea level (minus the annual cycle and inverse-barometer response) at Fremantle and Darwin harbours, *iv)* onshore and *v)* alongshore components of 60-day averaged NCEP-NCAR Reanalysis surface wind stress, averaged over the region indicated, *vi)* Reynolds monthly-averaged sea surface temperature, and *vii)* 8-day composite SeaWiFS estimates of surface chlorophyll-a.

Inter-annual variability
The number of model larvae settling each year was relatively constant (Fig. 14), compared with the five-fold difference between the observed puerulus settlements of 1996 and 1993 (Fig. 18). The modeled settlement did not correlate with the observations, and the ranking of the model years was sensitive to small changes of many of the model parameters. Even re-running the model with nothing changed but the random velocities could re-order the settlement rates. Some model runs gave settlement rates that correlated with the observed inter-annual variability, but no model runs gave the large observed differences between years.

The only model statistics that varied robustly between years were the number of model larvae exiting the model domain to the north (which happened early in the year), and the number rounding Cape Leeuwin and exiting to the east (later in the year). For example, in 1993, 40% of the year class (which was twice the usual number) of larvae exited north as a consequence of the weakened geostrophic flow that was indicated by low sea levels (Fig. 18). Summer south-easterly winds of early 1993 were no stronger than usual. Loss of larvae around Cape Leeuwin was negatively correlated with loss to the north. In 1996, 40% of the year class (again twice the usual number) were lost around Cape Leeuwin, and again, this was associated with an anomalous (strong) Leeuwin Current, as indicated by high sea level (Fig. 18). The wind in 1996 had an anomalously strong eastward component that drove a northward Ekman flux and north-eastward surface current. The effect of this on the model larvae was to keep them closer to the continental shelf, where the strongest southward flow occurred.

The number of late-stage model larvae left in the middle, adjacent to the adult population, was therefore relatively constant between years, as reflected, albeit more noisily, in the number of larvae modeled as settling.

The time scale over which all model larvae either left the model domain or settled was such that settlement of year classes did not overlap, except in 1994 when larval loss due to advection was so low that modeled puerulus settlement in 1995 was potentially augmented by settlement of the 1994 year class. However, the model explicitly excludes all other causes of larval loss such as predation and starvation, which might reduce the effect of prior year classes.

Sensitivity of results to parameter uncertainty
The observed rate of puerulus settlement in 1995 and 1996 was very high, but these were years when the model had many larvae rounding Cape Leeuwin. Were we either over-estimating the strength of the Leeuwin, under-estimating the effect of the summer surface wind drift northwards, or under-estimating the depth to which mid and late-stage larvae descend by day? Recall that the ‘standard’ model run employed the mean flow estimated by the global ocean model. If we instead used the mean flow computed from the hydrographic climatology, relative to either 300 or 1000 m, there was still no correlation of modeled and observed settlement rates, although the numbers exiting the model domain were slightly less.

Increasing the surface wind drift factor from 3.5% to 5% significantly reduced the number of larvae rounding Cape Leeuwin, and increased the number exiting north and exiting west, which was insignificant for the standard run. The numbers remaining in the middle and settling were less, and still constant across years. Conversely, reducing the surface wind drift factor to 2% slightly increased the number rounding Cape Leeuwin, at the expense of the number going north.

Increasing the mean depth to which mid and late-stage larvae descended by day from 70 m to 100 m had essentially no impact, which may reflect a failing of the global model to resolve the shear. Using the deeper hydrographic mean current field also had little influence. Attenuating the altimetric current at depth by 0.5 instead of 0.8 did not reduce the losses around Cape Leeuwin.

The importance of vertical migration
To investigate the importance of diurnal vertical migration, we performed experiments in which model larvae ascended for 0 or 16 h (instead of 8 h for the standard run). In the 0 h run, half (instead of 10%) of the model larvae rounded Cape Leeuwin by July under the influence of the Leeuwin Current. In the 16 h run, half (instead of 15%) of the model larvae exited the model domain to the north or west by April. The fraction of time spent near the surface was therefore a parameter to which the trajectories of the model larvae were very sensitive.

Metamorphosis and swimming

No experiments with the parameters controlling metamorphosis and settlement made significant changes to the inter-annual variations of modeled settlement. The eastward swimming speed (0.1 m/s) of the model puerulus was enough to give them an approximately 50% chance, for each year modeled, of reaching the 100 m isobath within one week.

Discussion

The present work was motivated by a desire to explore the hypothesis that inter-annual variations of transport of the phyllosoma larvae could be responsible for the observed correlation of coastal sea level with puerulus settlement. For our simulations, we used the most accurate velocity fields available, as distinct from the most detailed, which are now provided by the ROMS hydrodynamic model. The benefit of our approach was that the temporal variability of both the large-scale flows and mesoscale eddies was well represented for the particular year classes simulated. The principal drawback of this method, however, was that our representation of vertical shear was fairly crude, although we doubt it was limiting, given the gaps in our knowledge of the vertical migration behaviour of the larvae. The altimetric analysis had other weaknesses. One was that the flows over the continental shelf, especially the across-isobath component, were poorly represented. We think that this failing was unlikely to be limiting the model, compared with the crude algorithm for triggering metamorphosis to the puerulus. Poor resolution of sharp fronts was another weakness, the consequence of which was hard to anticipate, since it depended on whether the diurnal migrations of real larvae result in their crossing fronts.

The impact of the large sea level anomalies occurring during our study period was evident in the flow fields and subsequent movement of model larvae, but the number of late-stage larvae being transported to the shelf edge around the time of settlement did not vary nearly as much between years as did natural settlement on coastal collectors. For the presently-modeled settlement rate to correlate better with observations, the number of model larvae being carried around Cape Leeuwin needed to be lower in years of strong Leeuwin Current. The losses to the north in years of weak flow would then generate variability that would correlate with observed settlement.

Notwithstanding the model's deficiencies, the model's results were consistent with observed survival patterns, without 'tuning' its parameters away from literature-based estimates. The observed vertical migration balanced the north- and westward influence of the wind against the south- and eastward influence of the geostrophic flow. This is essentially the balance that has generally been assumed to exist (eg Pearce and Phillips, 1994), but which has not previously been evaluated quantitatively. We are not aware, in fact, of any species with such an extended pelagic larval phase, for which the mechanism for retention of a large proportion of hatched larvae within the range of the species has been quantitatively evaluated.

Benefits

This project was not designed to produce immediate, quantifiable benefits to the fishing industry. After seeing the work, however, long-liners have shown interest in using the altimetic current maps produced by CSIRO in real-time to help decide where to set their lines. The project was more designed to ensure long-term sustainable management than to increase fishing efficiency, so the direct beneficiaries of the work are fisheries scientists and managers. The benefits are that they now know much more about ocean currents off WA, and how larvae of western rock lobster manage to return to the coast in the presence of a current which one might expect to carry them all away. Scientists and managers are now one step closer to solving the riddle of why El Nino inflences western rock lobster catches. Managers have increased confidence that they are doing the right thing in attempting to promote egg production equally in all areas of the fishery.

Further Development

Our work suggests that the environmental factor directly responsible for the large variations observed of settlement of western rock lobster puerulus is one that correlates with sea level and was not included in the model. One such factor is temperature, which affects hatching (Aldrich, 1967), growth rate and survival (Chittleborough and Thomas, 1969, Marinovic, 1996) and is correlated with both sea level and puerulus settlement (Caputi *et al.*, 2001). Earlier hatching and faster development of larvae when the water is warmer would favour a greater proportion metamorphosing and settling before being carried south by the current. A second may be food availability. The advent of quantitative ocean colour imagery (see Figure 17 for an example image) in 1997 enables a representation of prey density to also be included in a model, once the relationship of surface chlorophyll-a with the feeding-depth abundance of preyed-upon creatures (which need to be identified) is known (if indeed there is one). Inspection of the few available years of SeaWiFS ocean colour images shows that while the winter chlorophyll-a density varied little between years, the density during the El-Nino summer of 1997-98 was low (see Fig. 18), potentially explaining the very low settlement rate in 1998 and encouraging further study. Figure 17 shows how great are the differences, between areas, of the amount of phytoplankton in the water. The mortality and growth rates of larvae are bound to be influenced by these differences. To incorporate this information into a larval advection model would seem to be the logical follow-on to the present work.

The present larval advection model had numerous simplifications and it is hard to know which was primarily responsible for its failure to reproduce the observed extent of inter-annual variability of puerulus settlement. One of these deficiencies was our lack of understanding of the cue to metamorphose from the final phyllosoma larval stage to the puerulus. Field studies of puerulus abundance are confounded by the strong currents over the continental slope, such that recently-metamorphosed pueruli occurring far offshore did not necessarily metamorphose there, or even in that water mass. Velocities of up to 1.5 m/s either shoreward or seaward need to be factored in the model to back-calculate the location of metamorphosis.

This project has produced a suite of tools with a wide range of potential applications. The CD-ROM (Appendix 4) was produced in order to encourage usage of these tools as well as being a means for disseminating the results of our use of them. The application to advection of western rock lobster larvae was the primary motive for the development of the tools, so that was where we focused attention in their application.

The larval advection model has also been used for salmon, pilchard and herring. The influence of the strong Leeuwin Current in 1996 is clear. We have not documented these results here, however, because they are only preliminary. We also note that the results are quite sensitive, as they were for western rock lobster, to the amount of time per day that larvae are assumed to be close to the surface. This information was available from the field for western rock lobster, but there is much greater uncertainty about it for these finfish species. To apply the model to other Australian lobster species would also be well worth doing.

Planned Outcomes

The first major output of the project was the development and validation of methods of inferring surface currents from satellite observations of sea level. Many seminars were given to encourage usage of these data, with the outcome being that the worth of the method is now quite widely recognized.

A more tangible output is the archive of ocean data assembled for the project. The outcome of this is that anyone with internet access can now find out, after just a few mouse clicks, what the ocean circulation actually was on any day from 1993 to 2000.

The output of the larval advection modeling was greater understanding of the crucial larval phase of Australia's most valuable single species fishery. The mystery of why El Nino has such a strong negative impact on the species was not solved, but further research into environmental influences on those larvae will doubtlessly build on the work reported here.

The result that probability of larval survival and recruitment to the fishery does not depend on hatching latitude was not unexpected, so management of the fishery with regard to emphasis on protecting certain areas over others has not changed.

Conclusion

The first objective of 'developing algorithms for the operational estimation of near surface temperatures and currents based on satellite altimetry and thermometry' was met, although we found that since the altimetry method worked so well on its own, the method proposed for using thermometry did not add any extra value. An alternative means of using thermometry was explored, but it remains in the development stage (see Appendix 3). The outcome of this work is described above.

The second objective of 'developing and testing a three-dimensional data assimilating model of ocean dynamics off Western Australia, to be run in hindcast mode, archiving

data for the last ten years' was met to the extent that the model was developed and tested. Since we found, however, that the model did not substantially improve upon the value of the data assimilated to it, we have only archived four years (1995-1998) of output (Appendix 5). We conclude that the sub-optimal 'blending' method that we proposed to use is unlikely to make the model add substantial value, for mesoscale applications like the present one, to the observations, so the much more computationally demanding variational methods will probably have to be used.

The third objective of 'to run tracking scenarios for rock lobster larvae to describe larval behaviour under different environmental conditions (extended to other larvae as time permits)' has been met. The six years simulated included good examples of both El Nino and La Nina conditions, so the fact that modeled settlement did not vary greatly was not for lack of variability in the ocean conditions. Otherwise, the modeling results are in agreement with (historical) observations of the rate at which larvae disperse in the ocean. The fact that relatively many model larvae remain in the region of the adult population, despite the existence of a strong southward flow, suggests that the model is a basically correct representation of nature, although it is bound to have shortcomings. The advection model was also run for several years for salmon, pilchard and herring, but we have not finished running the model with trial values for poorly-known parameters.

The final objective 'to provide advice on management issues that may be addressed by improved ocean understanding, such as the spawning locations of successful larvae, and correlations between larval success and ocean conditions' was met although the news was not good. We hoped that an improved forecast of larval settlement might result from a better understanding of the larval stage. This has not eventuated. Instead, our work concludes that one of the leading hypotheses for why sea level works as a predictor of larval settlement, ie by being an indicator of the strength of the current, is unlikely to be true. The section on Further Development outlines our suggestion for the direction that future research should take.

A reminder of the continued need for a process-based understanding of larval recruitment dynamics was provided by the failure of the statistical prediction of average settlement for 1998, when very poor larval settlement was observed. Was that because the breeding stock had become critically low? We know it wasn't because research data showed improvements in the size of the breeding stock brought about by the management package introduced in 1993.The puerulus settling in 1998 were hatched during an extremely intense El Nino, which normally results in poor settlement. The failure of the statistical prediction is possibly associated with the fact that the El Nino of 1997-98 reverted to La Nina extremely quickly, so April sea level, for example, retained no record of the El Nino. Further statistical analyses of the data sets now available should result in a new prediction scheme that correctly hindcasts the 1998 settlement. The role of research into the mechanisms responsible is to increase confidence that the skill of the statistical methods is not artificial.

References

Aldrich, F. (1967). Observations by the late F. Aldrich on Australian marine crayfish in captivity. *Western Australian Naturalist* **10,** 162-8.

Andrews, J. C. (1983). Ring structure in the poleward boundary current off western Australia. *Australian Journal of Marine and Freshwater Research* **34,** 547-61.

Caputi, N., Fletcher, W. J., Pearce, A. F. and Chubb, C. F. (1996). Effect of the Leeuwin Current on the recruitment of fish and invertebrates along the west Australian coast. *Marine and Freshwater Research* **47,** 147-55.

Caputi, N., Chubb, C. F. and Pearce, A. F. (2001). Environmental effects on the recruitment of the western rock lobster, *Panulirus cygnus.*. *Marine and Freshwater Research* (this issue).

Chittleborough, R. G., and Thomas, L. R. (1969). Larval ecology of the western Australian marine crayfish, with notes upon other panulirid larvae from the eastern Indian Ocean. *Australian Journal of Marine and Freshwater Research* **20,** 199-223.

Chiswell, S. M. and Booth, J. D. (1999). Rock Lobster *Jasus Edwardsii* larval retention by the Wairarapa Eddy off New Zealand. *Marine Ecology Progress Series* **183,** 227-40.

Chubb, C. F. (1991). Measurement of spawning stock levels for the western rock lobster, *Panulirus cygnus. Revista de Investigaciones Marinas* **12,** 223-33.

Cresswell, G. R. and Golding, T. J. (1980). Observations of a south-flowing current in the southeastern Indian Ocean. *Deep Sea Research* **27A,** 449-66.

Godfrey, J. S. and Ridgway, K. R. (1985). The large-scale environment of the poleward-flowing Leeuwin Current, western Australia: Longshore steric height gradients, wind stresses and geostrophic flow. *Journal of Physical Oceanography* **15,** 481-95.

Griffin, D. A. and Middleton, J. H. (1991). Local and remote wind forcing of New South Wales inner shelf currents and sea level. *Journal of Physical Oceanography* **21,** 304-22.

Hamon, B. V. and Cresswell, G. R. (1972). Structure functions and intensities of ocean circulation off east and west Australia. *Australian Journal of Marine and Freshwater Research* **23,** 99-103.

Hofmann, E. E., Hedstrom, K. S., Moisan, J. R., Haidvogel, D. B. and Mackas, D. L. (1991). Use of Simulated Drifter Tracks to Investigate General Transport Patterns and Residence Times in the Coastal Transition Zone. *Journal of Geophysical Research* **96,** 15041-52.

Incze, L. S. and Naimie, C. E. (2000). Modelling the transport of lobster *(Homarus americanus)* larvae and postlarvae in the Gulf of Maine. *Fisheries Oceanography* **9,** 99-113.

Kalnay, E., Kanamitsu, M., Kistler, R., Collins, W., Deaven, D., Gandin, L., Iredell, M., Saha, S., White, G., Woollen, J., Zhu, Y., Chelliah, M., Ebisuzaki, W., Higgins, W., Janowiak, J., Mo, K. C., Ropelewski, C., Wang, J., Leetmaa, A., Reynolds, R., Jenne, R. and Joseph, D. (1996). The NCEP/NCAR 40-year reanalysis project. *Bulletin of the American Meteorological Society* **77,** 437-71.

Katz, C. H., Cobb, J. S. and Spaulding, M. (1994). Larval behavior, hydrodynamic transport, and potential offshore-to-inshore recruitment in the American lobster *Homarus americanus. Marine Ecology Progress Series* **103,** 265-73.

Lemmens, J. W. T. J. (1994). Biochemical evidence for absence of feeding in puerulus larvae of the western rock lobster *Panulirus cygnus* (Decapoda: Palinuridae). *Marine Biology* **118,** 383-91.

Lenanton, R. C., Joll, L., Penn, J. and Jones, K. (1991). The influence of the Leeuwin Current on coastal fisheries of Western Australia. In: Proceedings of the Leeuwin Current Symposium, Perth, 16 March 1991. *Journal of the Royal Society of Western Australia* **74,** 101-14.

Le Traon, P.-Y. and Hernandez, F. (1992). Mapping the oceanic mesoscale circulation: Validation of satellite altimetry using surface drifters. *Journal of Atmospheric and Oceanic Technology* **9**, 687-98.

Marinovic, B. B. (1996). Behavioural and physiological investigations with respect to light and temperature on the phyllosoma larvae of the western rock lobster *Panulirus cygnus* George, 1962. Ph.D.thesis, University of Western Australia.

Millan-Nunez, R., Alvarez-Borrego, S. and Trees, C. C. (1997). Modeling the vertical distribution of chlorophyll in the California Current System. *Journal of Geophysical Research* **102,** 8587-95.

Pattiaratchi, C., Pearce, A. F., Hick, P., and Ong, C. (2000). Export of productive waters from the west Australian continental shelf by the Leeuwin Current. *Marine and Freshwater Research,* submitted.

Pearce, A. F. and Phillips, B. F. (1988). ENSO events, the Leeuwin Current, and larval recruitment of the western rock lobster. *Journal du Conseil International pour l'Exploration de la Mer* **45,** 13-21.

Pearce, A. F. and Griffiths, R. W. (1991). The mesoscale structure of the Leeuwin Current : a comparison of laboratory model and satellite images. *Journal of Geophysical Research* **96,** 16739-57.

Pearce, A. F. and Phillips, B. F. (1994). Oceanic processes, puerulus settlement and recruitment of the western rock lobster *Panulirus cygnus* . In 'The Biophysics of

Marine Larval Dispersal'. (Eds P.W. Sammarco, and M.L. Heron.). American Geophysical Union, Coastal and Estuarine Studies **45**, 352pp.

Phillips, B. F. (1975). The effect of water currents and the intensity of moonlight on catches of the puerulus larval stage of the western rock lobster. *Report of the Division of Fisheries and Oceanography, CSIRO Australia*, No. 63.

Phillips, B. F. (1981). The circulation of the southeastern Indian Ocean and the planktonic life of the western rock lobster. *Oceanography and Marine Biology Annual Review* **19,** 11-39.

Phillips, B. F. (1986). Prediction of commercial catches of the Western Rock Lobster *Panulirus cygnus* George. *Canadian Journal of Fisheries and Aquatic Sciences* **43,** 2126-30.

Phillips, B. F. and Olsen, L. (1975). Swimming behaviour of the puerulus larvae of the Western Rock Lobster. *Australian Journal of Marine and Freshwater Research* **26,** 415-7.

Phillips, B. F., Rimmer, D.W. and Reid, D. D. (1978). Ecological investigations of the late-stage phyllosomata and puerulus larvae of the western rock lobster *Panulirus longipes cygnus*. *Marine Biology* **45,** 347-57.

Phillips, B. F. and Pearce, A. F. (1997). Spiny lobster recruitment off Western Australia. *Bulletin of Marine Science* **61,** 21-41.

Pollard, R. T. and Millard, R. C. (1970). Comparison between observed and simulated wind-generated inertial oscillations. *Deep Sea Research* **17,** 813-21.

Polovina, J. J., Kleiber, P. and Kobayashi, D. R. (1999). Application of Topex/Poseidon satellite altimetry to simulate transport dynamics of larvae of the spiny lobster (*Panulirus marginatus*), in the Northwestern Hawaiian Islands, 1993-96. *Fisheries Bulletin* **97,** 132-43.

Rimmer, D. W. and Phillips, B. F. (1979). Diurnal Migration and vertical distribution of phyllosomata larvae of the western rock lobster *Panulirus cygnus*. *Marine Biology* **54,** 109-24.

Rimmer, D. W. (1980). Spatial and temporal distribution of early-stage phyllosomata of western rock lobster, *Panulirus cygnus*. *Australian Journal of Marine and Freshwater Research* **31,** 485-97.

Ritz, D. A. (1972). Factors affecting the distribution of rock-lobster larvae (*Panulirus longipes cygnus*), with reference to variability of plankton-net catches. *Marine Biology* **13,** 309-17.

Schiller, A., Godfrey, J. S., McIntosh, P. C., Meyers, G. and Fiedler, R. (2000). Interannual dynamics and thermodynamics of the Indo-Pacific Oceans. *Journal of Physical Oceanography* **30,** 987-1012.

Appendix 1: Intellectual Property

No intellectual property arising from this project is envisaged to have commercial value.

Appendix 2: Staff

Suzy Ayvazian, Fisheries WA
Ian Barton, CSIRO
Nick Caputi, Fisheries WA
Chris Chubb, Fisheries WA
Jeff Dunn, CSIRO
Dan Gaughan, Fisheries WA
David Griffin, CSIRO
Rod Lenanton, Fisheries WA
Jim Mansbridge, CSIRO
Alan Pearce, CSIRO
Chris Rathbone, CSIRO
Ken Ridgway, CSIRO
Andreas Schiller, CSIRO
Paul Tildesley, CSIRO
Angela Way, CSIRO
Neil White, CSIRO
John Wilkin, NIWA

Appendix 3: Ocean currents from successive satellite images: the reciprocal filtering technique.

This paper has been submitted to the Journal of Atmospheric and Oceanic Technology. Contact Dr Ian Barton at CSIRO Marine Research to obtain a copy, or check the journal.

Appendix 4: WA ocean movies 1993-2000.

This is a CD-ROM published by CSIRO Marine Research. Contact Alan Pearce, David Griffin or the libraries at CSIRO Marine Research for a copy, or visit www.marine.csiro.au/~griffin/WACD.

Appendix 5: WA ocean model movies 1995-1998.

This is a CD-ROM not formally published, but available from David Griffin, CSIRO Marine Research.